Model Predictive Control of Power Electronic Systems: Methods, Results, and Challenges

Petros Karamanakos, *Senior Member, IEEE*, Eyke Liegmann, *Student Member, IEEE*, Tobias Geyer, *Senior Member, IEEE*, and Ralph Kennel, *Senior Member, IEEE*

***Abstract*—Model predictive control (MPC) has established itself as a promising control methodology in power electronics. This survey paper highlights the most relevant MPC techniques for power electronic systems. These can be classified into two major groups, namely, MPC without modulator, referred to as direct MPC, and MPC with a subsequent modulation stage, known as indirect MPC. Design choices and parameters that affect the system performance, closed-loop stability and controller robustness are discussed. Moreover, solvers and control platforms that can be employed for the real-time implementation of MPC algorithms are presented. Finally, the MPC schemes in question are assessed, among others, in terms of design and computational complexity, along with their performance and applicability depending on the power electronic system at hand.**

***Index Terms*—Power electronic systems, power converters, ac drives, model predictive control (MPC), direct control, indirect control, modulator, integer programming, quadratic programming.**

I. Introduction

MODEL predictive control (MPC) [1], [2] emerged as a time-domain control strategy in the 1960s [3]–[6]. Over the next decade, it established itself as an effective control strategy for nonlinear, multiple-input multiple-output (MIMO), constrained plants with complex dynamics predominantly used in the process industry. Later on, and owing to its versatility, MPC paved its way in numerous other industries, including, but not limited to, the mining, automotive and aerospace industries [7].

In the 1980s, the power electronics community started investigating the potential of MPC [8], [9], but the meager computational resources of the time combined with the emergence of power semiconductor devices that allowed higher switching frequencies limited its applicability and perceived benefits. After a hiatus in the development of MPC-based algorithms for power electronic systems for about two decades, the ever-increasing computational power and the subsequent advent of powerful microprocessors instigated the resurgence of interest in MPC for power electronics in the 2000s [10]–[13]. Several variants of MPC have thenceforth been developed for and implemented in power converters used in applications such as electrical drives, static synchronous compensators (STATCOMs), high-voltage dc (HVDC) systems, flexible ac transmission systems (FACTS), and uninterruptible power supplies (UPS), to name a few [14]–[20].

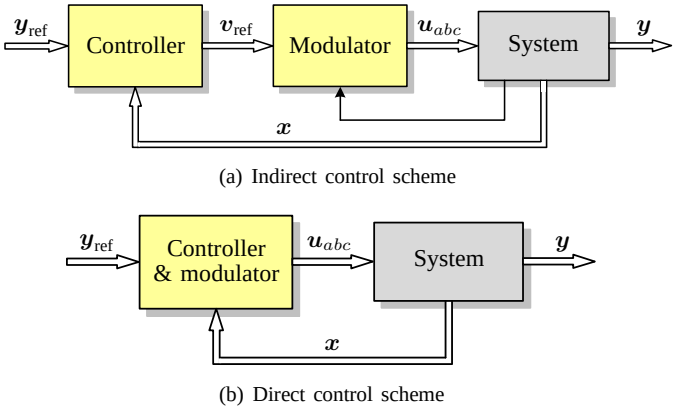

(a) Indirect control scheme

(b) Direct control scheme

Fig. 1: Main controller structures.

MPC schemes for power electronics can be classified into two main categories depending on whether they employ a separate modulator or not. In the former case, MPC is implemented as an *indirect* controller, i.e., the controller computes the modulating signal/duty ratio which is fed into a modulator for generation of the switching commands, see Fig. 1(a). Hence, the control action is a real-valued vector. On the other hand, when MPC is designed as a *direct* controller the control and modulation problems are formulated and solved in one computational stage, thus, not requiring a dedicated modulator, see Fig. 1(b). Consequently the elements of the control input vector are the switching signals, implying that it is an integer vector.

The aforementioned MPC algorithms can be further divided into smaller groups as shown in Fig. 2. Direct MPC-based schemes include controllers with reference tracking, hysteresis bounds and implicit modulator. Direct MPC with reference tracking—also known as finite control set MPC (FCS-MPC)—is the method most favored in academia due to its well-reported advantages such as its intuitive design procedure and straightforward implementation [13], [21]–[32]. The aim is to achieve regulation of the output variables along their reference trajectories by manipulating the converter switches, and thus directly affecting their evolution. This variant of direct MPC, however, comes with pronounced computational complexity which can potentially lead to computationally intractable optimization problems, as discussed later in the paper. Moreover, researchers often—knowingly or not—resort

P. Karamanakos is with the Faculty of Information Technology and Communication Sciences, Tampere University, 33101 Tampere, Finland; e-mail: p.karamanakos@ieee.org

E. Liegmann and R. Kennel are with the Chair of Electrical Drive Systems and Power Electronics, Technische Universität München, Munich 80333, Germany; e-mail: eyke.liegmann@tum.de, ralph.kennel@tum.de

T. Geyer is with ABB System Drives, 5300 Turgi, Switzerland; e-mail: t.geyer@ieee.org

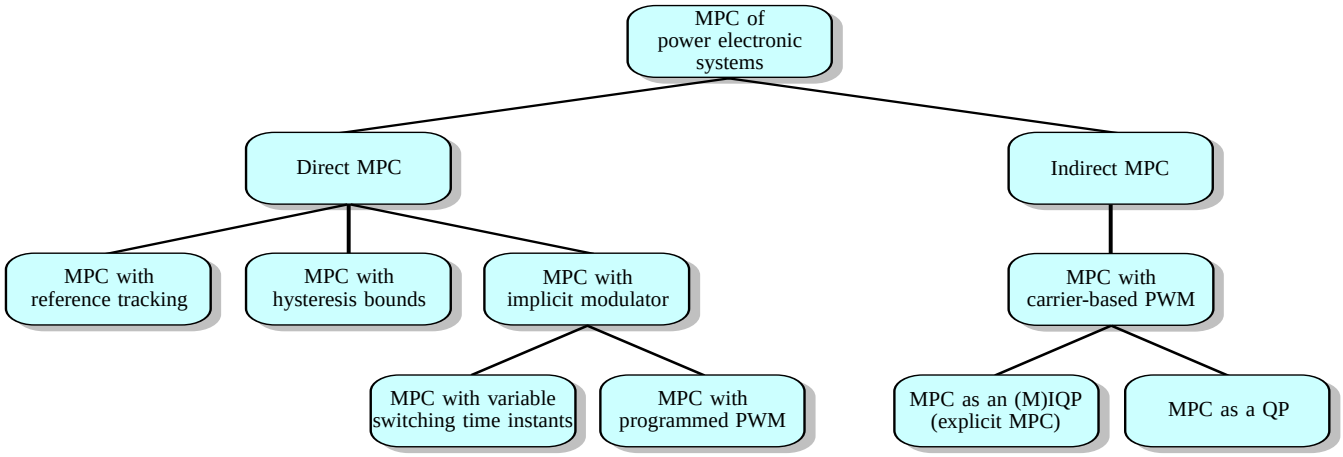

Fig. 2: Classification of MPC methods for power electronic systems.

to design simplifications that detract from its effectiveness and result in inferior performance compared with conventional control techniques, see [33] for more details.

Direct MPC with hysteresis bounds was the first rudimentary version of this type of controllers developed for power electronic converters [8], [34]–[37]. This algorithm employs hysteresis bounds within which the variables of interest, such as the stator currents, or the electromagnetic torque and stator flux magnitude of a machine, need to be constrained. Later, more sophisticated derivatives were devised which adopt a variety of optimization criteria and/or nontrivial prediction horizons [38]–[46]. Moreover, the versatility of the method in discussion allowed for different types of hysteresis bounds that affect the system performance in terms of, e.g., harmonic distortions or switching losses [34], [47], [48].

Finally, the third group of direct MPC strategies can be further divided into two subgroups. The first one includes methods that manipulate not only the switching signals, but also their application time in an attempt to emulate the behavior of pulse width modulation (PWM) techniques. More specifically, these methods—and in contrast to the aforementioned direct MPC strategies—introduce the concept of variable switching time instants by changing the state of the switches at any time instant within the sampling interval. This is done by computing both the optimal switch positions and the associated duty cycles [49]–[60]. In doing so, higher granularity of switching is introduced enabling the reduction of the harmonic distortion in the variables of concern. Moreover, some of these methods achieve operation of the power converter at a fixed switching frequency, thus resulting in deterministic switching losses [51], [53], [56], [59]–[68].

The second group consists of direct MPC methods that are combined with programmed PWM [69], i.e., modulation methods that forgo a fixed modulation interval. The switching pattern and the switching instants are computed offline based on some optimization criteria, such as minimization of the current total harmonic distortion (THD) and/or the elimination of specific harmonics. Programmed PWM is implemented in the form of selective harmonic elimination (SHE) [70], [71], or optimized pulse patterns (OPPs) [72], [73]. The idea of manipulation of the switching instants of OPPs in a predictive fashion was introduced in [74], [75], and [76], [77], for stator current and stator flux reference trajectory tracking, respectively. These methods, however, lack the receding horizon policy and do not distinguish between the fundamental and the ripple components, thus complicating the observer design [78]. To address these issues, more sophisticated MPC algorithms for the control of OPPs deemed necessary, leading to the methods presented in [79]–[81]. Moreover, SHE with MPC is presented, e.g., in [82]–[84]. Owing to the nature of the programmed modulation methods these MPC-based strategies achieve very low harmonic distortions, but they are fairly elaborate since fast closed-loop control is challenging.

As for the indirect MPC algorithms, these are methods that employ carrier-based PWM, such as sinusoidal PWM (SPWM) or space vector modulation (SVM) [69], [85], [86]. Depending on the formulation of the MPC problem, i.e., if it is a (mixed) integer quadratic program ((M)IQP) or merely a (constrained or unconstrained) quadratic program (QP), these methods can be split into two groups. The first subgroup of controllers uses explicit MPC to solve the (M)IQP. Specifically, the optimization problem underlying MPC is solved offline for all possible states of the power electronic system. As a result, the state-feedback control law is obtained and stored in look-up tables [87], [88], while methods, such as branch-and-bound (BnB) strategies [89], are employed in real time to acquire the solution in a computationally efficient manner. Finally, the control input, e.g., the modulating signal or the duty cycle, is fed into a modulator, which in turn generates the switching commands [90]–[98]. Explicit MPC schemes, however, are ill-suited for problems of higher dimensions since the memory requirements for storing the explicit control law increase exponentially with the problem size and complexity.

Finally, the second group of indirect MPC methods totally masks the switching nature of the power converter. In doing so, the optimization problem can be cast as a constrained or unconstrained QP. The former is relatively easier—compared to the aforementioned methods—to solve in real time owing to the several existing off-the-self solvers, as discussed later in this survey [99]–[104]. The latter allows for an analytical solution of the MPC problem [105]–[108]. This means that the state-feedback control law can be computed offline, thus

greatly simplifying the implementation of such controllers.

In the sequel of this paper, the main characteristics of direct and indirect MPC methods are discussed. Different design choices for formulating the optimization problem underlying MPC are presented. Furthermore, tuning parameters, such as weighting factors, the prediction horizon length as well as the sampling interval, and their effect on the system performance are summarized along with important aspects of MPC strategies, namely their robustness and closed-loop stability performance. Moreover, solvers for the mixed-integer programs and QPs as well as the associated challenges of the real-time implementation of MPC algorithms on embedded systems are analyzed. In addition, a brief assessment of the discussed MPC methods is provided and their main strong points and weaknesses are identified. Finally, the survey reflects on the main contemporary aspects and research directions of MPC.

This survey paper is structured as follows. The main ingredients that all MPC-based controllers share in common are summarized in Section II. Design considerations and their implications on the performance of the power electronic system are discussed in Section III. Section IV presents implementation-related issues and challenges of direct and indirect MPC, whereas Section V assesses their performance. Finally, Section VI confers on the current trends of MPC in academia and industry, and conclusions are drawn in Section VII.

II. Model Predictive Control: Features and Operating Principle

Three are the basic pillars of MPC, namely the mathematical model of the plant, the constrained (linear or nonlinear) optimal control problem, and the receding horizon policy [2]. In the sequel of this section, the aforementioned fundamental components of MPC are briefly described.

A. Mathematical Model of the Plant

MPC, as indicated by its name, is a model-based control method; an accurate model of the system is required for meaningful predictions of its future behavior, especially in disciplines like power electronics where control actions are taken within a few tens of microseconds. The vast majority of models of power electronic systems that serve as prediction models for MPC have three characteristics in common. First, they are based on the continuous-time state-space model. To derive the latter the variables that fully describe its dynamics are chosen and aggregated to the state vector $\boldsymbol{x} \in \mathbb{R}^{n_x}$. Typically, such variables are those that relate to the energy storage elements of the system, such as inductor currents, capacitor voltages, etc. Moreover, the n_u manipulated variables which affect the future behavior of the system need to be selected. In case of direct MPC, these can represent the switch positions, whereas when indirect MPC is of concern they can model the modulating signal. Assuming, without loss of generality, a three-phase system ($n_u = 3$), the vector of manipulated variables in case of direct MPC is integer valued, i.e.,

$$\boldsymbol{u} = [u_a \ u_b \ u_c]^T \in \boldsymbol{\mathcal{U}}_\delta = \mathcal{U}_\delta \times \mathcal{U}_\delta \times \mathcal{U}_\delta = \mathcal{U}_\delta^3 \subset \mathbb{Z}^3 \,. \quad (1)$$

On the other hand, a real-valued input vector results with indirect MPC, i.e.,

$$\boldsymbol{u} = [u_a \ u_b \ u_c]^T \in \boldsymbol{\mathcal{U}}_\kappa = [-1, 1]^3 \subset \mathbb{R}^3 \,. \quad (2)$$

As a result, the continuous-time state-space model takes the form

$$\frac{\mathrm{d}\boldsymbol{x}(t)}{\mathrm{d}t} = \boldsymbol{f}_c\big(\boldsymbol{x}(t), \boldsymbol{u}(t)\big) \quad (3a)$$

$$\boldsymbol{y}(t) = \boldsymbol{g}_c\big(\boldsymbol{x}(t)\big) \,, \quad (3b)$$

where $\boldsymbol{y} \in \mathbb{R}^{n_y}$ is the vector of the n_y output variables of the system which are chosen based on the application in question. Typical output variables along with relevant applications are shown in Table I. Moreover, $\boldsymbol{f}_c(\star) : \mathbb{R}^{n_x} \times \boldsymbol{\mathcal{U}}_\epsilon \to \mathbb{R}^{n_x}$ and $\boldsymbol{g}_c(\star) : \mathbb{R}^{n_x} \to \mathbb{R}^{n_y}$ are the state-update[1] and output functions, respectively, where $\epsilon \in \{\kappa, \delta\}$. In most cases, the power electronic system (3) is a linear or bilinear system [109].[2] In the former case, the continuous-time state-space model takes the form

$$\frac{\mathrm{d}\boldsymbol{x}(t)}{\mathrm{d}t} = \boldsymbol{A}_c\boldsymbol{x}(t) + \boldsymbol{B}_c\boldsymbol{u}(t) \quad (4a)$$

$$\boldsymbol{y}(t) = \boldsymbol{C}_c\boldsymbol{x}(t) \,, \quad (4b)$$

where $\boldsymbol{A}_c \in \mathbb{R}^{n_x \times n_x}$, $\boldsymbol{B}_c \in \mathbb{R}^{n_x \times n_u}$, and $\boldsymbol{C}_c \in \mathbb{R}^{n_y \times n_x}$ are the system, input, and output matrices respectively. These matrices can be either time-invariant or time-varying, depending on the case study. On the other hand, for bilinear systems the state-update function is of the form [110]–[112]

$$\boldsymbol{f}_c\big(\boldsymbol{x}(t), \boldsymbol{u}(t)\big) = \big(\boldsymbol{A}_{c1} + \boldsymbol{A}_{c2}\boldsymbol{u}(t)\big)\boldsymbol{x}(t) + \boldsymbol{B}_c\boldsymbol{u}(t) \,.$$

Second, the modeling of three-phase systems is commonly performed in a two-dimensional rotating or stationary reference plane. Such a mapping—inherited by linear control methods where the aim is to achieve decoupling of the control loops—is realized by transforming any variable $\boldsymbol{\xi}_{abc} = [\xi_a \ \xi_b \ \xi_c]^T$ in the three-phase (abc) system into a two-dimensional variable via the matrix

$$\boldsymbol{K}(\varphi) = \frac{2}{3}\begin{bmatrix} \cos\varphi & \cos\big(\varphi - \frac{2\pi}{3}\big) & \cos\big(\varphi + \frac{2\pi}{3}\big) \\ -\sin\varphi & -\sin\big(\varphi - \frac{2\pi}{3}\big) & -\sin\big(\varphi + \frac{2\pi}{3}\big) \end{bmatrix} ,$$

where φ is the angle between the direct axis of the orthogonal plane and the a-axis of the three-phase system. Hence, for a reference plane rotating with angular speed ω_{fr}—the so-called dq-plane—the transformation is of the form

$$\boldsymbol{\xi}_{dq} = \boldsymbol{K}(\varphi)\boldsymbol{\xi}_{abc} \,,$$

where $\boldsymbol{\xi}_{dq} = [\xi_d \ \xi_q]^T$. When $\omega_{\mathrm{fr}} = 0$, i.e., the plane is stationary (known as the $\alpha\beta$-plane), the performed mapping to the variable $\boldsymbol{\xi}_{\alpha\beta} = [\xi_\alpha \ \xi_\beta]^T$ is

$$\boldsymbol{\xi}_{\alpha\beta} = \boldsymbol{K}(0)\boldsymbol{\xi}_{abc} \,.$$

[1] In presence of external disturbances, function $\boldsymbol{f}_c(\star)$ has as additional argument the vector of disturbances $\boldsymbol{d} \in \mathbb{R}^{n_d}$. For sake of simplicity, but without loss of generality, it is assumed that $\boldsymbol{d} = \boldsymbol{0}$ in the sequel of the paper.

[2] It is worth mentioning that even if the state-update function $\boldsymbol{f}_c(\star)$, see (3a), can be linear/bilinear, the output function $\boldsymbol{g}_c(\star)$, see (3b), can still be nonlinear since output variables, such as the flux magnitude, electromagnetic torque, real and reactive power, etc., represent a nonlinear combination of the state variables.

TABLE I: Typical output variables in power electronic systems.

Application	Output variable	Symbol	
Electrical drives	Stator current or flux	$\boldsymbol{i}_s$ or $\boldsymbol{\psi}_s$	[26], [113]
Electrical drives	Electromagnetic torque, stator or rotor flux magnitude	T_e, Ψ_s or Ψ_r	[24], [114], [115]
Neutral point clamped converters	Load current, neutral point potential	$\boldsymbol{i}_o$, v_n	[21]
Cascaded H-bridge converters	Load current, cell capacitor voltage	$\boldsymbol{i}_o$, v_c	[116], [117]
Active front-end rectifiers	Real and reactive power, dc-link voltage	P, Q, v_{dc}	[22], [23], [118]
Current-source rectifiers	Reactive power, dc-link current	Q, i_{dc}	[119]
Converters with filters	Converter current, filter capacitor voltage, load current	$\boldsymbol{i}_{\text{conv}}$, $\boldsymbol{v}_c$, $\boldsymbol{i}_o$	[120], [121]
UPS systems	Filter capacitor/load voltage	$\boldsymbol{v}_c$	[122]
Modular multilevel converters	Branch currents, module capacitor voltages, load current	i_x, v_x ($x \in \{1, 2, \ldots, 6\}$), $\boldsymbol{i}_o$	[29], [123]
Matrix converters	Input current or reactive power, load current	$\boldsymbol{i}_i$ or Q_i, $\boldsymbol{i}_o$	[65], [66], [124], [125]
Impedance-source converters	Dc-side inductor current, capacitor voltage, load current	i_L, v_c, $\boldsymbol{i}_o$	[126], [127]

TABLE II: Discretization methods used in MPC for power electronics.

Method	Form	Linear form	
Forward Euler	$\boldsymbol{x}(k+1) = \boldsymbol{x}(k) + T_s \boldsymbol{f}_c\Big(\big(\boldsymbol{x}(k), \boldsymbol{u}(k)\big), kT_s\Big)$	$\boldsymbol{x}(k+1) = (\boldsymbol{I} + T_s \boldsymbol{A}_c)\boldsymbol{x}(k) + T_s \boldsymbol{B}_c \boldsymbol{u}(k)$	[13], [21], [22]
Backward Euler	$\boldsymbol{x}(k+1) = \boldsymbol{x}(k) + T_s \boldsymbol{f}_c\Big(\big(\boldsymbol{x}(k+1), \boldsymbol{u}(k+1)\big), (k+1)T_s\Big)$	$\boldsymbol{x}(k+1) = \boldsymbol{x}(k) + T_s\big(\boldsymbol{A}_c \boldsymbol{x}(k+1) + \boldsymbol{B}_c \boldsymbol{u}(k+1)\big)$	[27], [98], [128]
Exact		$\boldsymbol{x}(k+1) = \mathrm{e}^{\boldsymbol{A}_c T_s} \boldsymbol{x}(k) + \Big(\int_0^{T_s} \mathrm{e}^{\boldsymbol{A}_c \tau} \mathrm{d}\tau \boldsymbol{B}_c\Big) \boldsymbol{u}(k)$	[26], [129], [130]

Finally, since MPC is a discrete-time controller, the continuous-time system (3) needs to be discretized

$$\boldsymbol{x}(k+1) = \boldsymbol{f}\big(\boldsymbol{x}(k), \boldsymbol{u}(k)\big) \tag{5a}$$

$$\boldsymbol{y}(k) = \boldsymbol{g}\big(\boldsymbol{x}(k)\big)\,, \tag{5b}$$

where $k \in \mathbb{N}$ indicates the discrete time step. To this end, forward Euler, backward Euler or exact discretization is most commonly employed [131], see Table II. The first two are popular because they are computationally cheap, thus, they do not increase the—already pronounced—computational load of MPC. However, the accuracy of both methods deteriorates as the sampling interval T_s increases, while forward Euler can also exhibit stability issues [131, Chapter 5]. On the other hand, exact discretization provides as precise a representation of the continuous-time dynamics as possible, but at the cost of higher computational complexity. Moreover, it is worth mentioning that the latter method is applicable only to linear time-invariant systems.

B. MPC Problem

The aim of MPC is to find the sequence of manipulated variables that achieve the most desired system behavior—as defined by an objective function—within a finite-time interval. To do so, first the aforementioned sequence is defined over a finite horizon of $N_p \in \mathbb{N}^+$ time steps as

$$\boldsymbol{U}(k) = \begin{bmatrix} \boldsymbol{u}^T(k) & \boldsymbol{u}^T(k+1) & \ldots & \boldsymbol{u}^T(k+N_p-1) \end{bmatrix}^T \in \mathbb{U}\,, \tag{6}$$

where $\mathbb{U} = \boldsymbol{\mathcal{U}}_\epsilon^{N_p}$. As can be deduced from (5), the future behavior of the power electronic system can be predicted over the prediction horizon based on $\boldsymbol{U}(k)$ and the present state $\boldsymbol{x}(k)$.

In a following step, the optimal control problem underlying MPC is formulated based on the chosen control objectives. To this aim, an objective function $J : \mathbb{R}^{n_x} \times \boldsymbol{\mathcal{U}}_\epsilon \to \mathbb{R}^+$ of the form

$$J\big(\boldsymbol{x}(k), \boldsymbol{U}(k)\big) = \sum_{\ell=k}^{k+N_p-1} J^\dagger\big(\boldsymbol{x}(\ell+1), \boldsymbol{u}(\ell)\big)\,, \tag{7}$$

is formulated that captures and quantifies the control objectives. Some common objective functions are presented in Table III in order of increasing design complexity. As can be seen, design choices relate to the norm used for the stage cost function $J^\dagger(\star)$, e.g., the ℓ_1- or ℓ_2-norm,[3] single or multiple output tracking,[4] the penalization (or not) of the control input, the length of the horizon, the use of a terminal state constraint, etc. Such issues are briefly discussed in Section III, whereas they are analyzed in more detail in [33].

Before formulating the optimization problem explicit constraints can be imposed on the variables of interest. Such restrictions can be implemented in the form of either *hard* or *soft* constraints. The former often represent physical limitations (e.g., on the control input, as indicated by (1) and (2)) and thus cannot be violated in any way. The latter, on the other hand, can be interpreted as protection mechanisms that enable the controller to operate the system within its safety limits. As such, they are imposed on the system state and, although they can be violated, effort should be put into avoiding such violations. To do so, the degree of their violation, usually modeled by slack variables, needs to be minimized [1].

[3]The ℓ_p-norm of a vector $\boldsymbol{\xi} \in \mathbb{R}^n$ is defined as $\boldsymbol{\xi} = (|\xi_1|^p + |\xi_2|^p + \ldots + |\xi_n|^p)^{1/p}$, for $p \geq 1$.

[4]Note that in case the output variables are of different quantities, e.g., currents, voltages, etc., and prioritization among them is required, then the ℓ_1- and ℓ_2-norms can appear in the "weighted" form $\|\boldsymbol{\Lambda}\boldsymbol{\xi}\|_p^p$, where $\boldsymbol{\xi} \in \mathbb{R}^{n_y}$, and $\boldsymbol{\Lambda} = \mathrm{diag}(\lambda_1, \lambda_2, \ldots, \lambda_{n_y})$ is a diagonal, positive (semi)definite weighting matrix, with $\lambda_i \in \mathbb{R}^+$, $i = 1, \ldots, n_y$. Specifically, for $p = 1$, the "weighted" ℓ_1-norm is of the form $\|\boldsymbol{\Lambda}\boldsymbol{\xi}\|_1 = \sum_{i=1}^{n_y} \lambda_i |\xi_i|$ [132], and for $p = 2$, the "weighted" ℓ_2-norm becomes $\|\boldsymbol{\Lambda}\boldsymbol{\xi}\|_2^2 = \sum_{i=1}^{n_y} \lambda_i^2 \xi_i^2 = \|\boldsymbol{\xi}\|_{\boldsymbol{Q}}^2$, where $\boldsymbol{Q} = \mathrm{diag}(q_1, q_2, \ldots, q_{n_y})$ with $q_i = \lambda_i^2$.

TABLE III: Common objective functions used in MPC for power electronics.

Expression	Features	
$J_1 = \|\boldsymbol{u}(k) - \boldsymbol{u}(k-1)\|_1$	Control effort penalization, one-step horizon, ℓ_1-norm	[39]
$J_2 = \|\boldsymbol{y}_{\text{err}}(k+1)\|_1$	Output reference tracking ($\boldsymbol{y}_{\text{err}} = \boldsymbol{y}_{\text{ref}} - \boldsymbol{y}$), ℓ_1-norm	[13]
$J_3 = \|\boldsymbol{y}_{\text{err}}(k+1)\|_2^2$	ℓ_2-norm	[122]
$J_4 = \|\boldsymbol{\Lambda}\boldsymbol{y}_{\text{err}}(k+1)\|_1$	Multiple outputs ($\boldsymbol{\Lambda} \succ \boldsymbol{0}$), one-step horizon, ℓ_1-norm	[24]
$J_5 = \|\boldsymbol{y}_{\text{err}}(k+1)\|_{\boldsymbol{Q}}^2$	Multiple outputs ($\boldsymbol{Q} \succ \boldsymbol{0}$), one-step horizon, ℓ_2-norm	[133]
$J_6 = \|\boldsymbol{y}_{\text{err}}(k+1)\|_1 + \lambda_u\|\Delta\boldsymbol{u}(k)\|_1$	$\Delta\boldsymbol{u}(k) = \boldsymbol{u}(k) - \boldsymbol{u}(k-1)$, control effort penalization ($\lambda_u > 0$)	[21]
$J_7 = \|\boldsymbol{y}_{\text{err}}(k+1)\|_2^2 + \lambda_u\|\Delta\boldsymbol{u}(k)\|_2^2$	Control effort penalization ($\lambda_u > 0$), ℓ_2-norm	[128]
$J_8 = \sum_{\ell=k}^{k+N_p-1} \|\Delta\boldsymbol{u}(\ell)\|_1$	Control effort penalization, multistep horizon ($N_p > 1$)	[46]
$J_9 = \sum_{\ell=k}^{k+N_p-1} \|\boldsymbol{y}_{\text{err}}(\ell+1)\|_2^2 + \lambda_u\|\Delta\boldsymbol{u}(\ell)\|_2^2$	Output reference tracking, $N_p > 1$, $\lambda_u > 0$	[26]
$J_{10} = \sum_{\ell=k}^{k+N_p-1} \|\boldsymbol{y}_{\text{err}}(\ell+1)\|_{\boldsymbol{Q}}^2 + \lambda_u\|\Delta\boldsymbol{u}(\ell)\|_2^2$	Multiple outputs ($\boldsymbol{Q} \succeq \boldsymbol{0}$)	[134]
$J_{11} = \|\boldsymbol{y}_{\text{err}}(k+N_p)\|_{\boldsymbol{R}}^2 + \sum_{\ell=k}^{k+N_p-1} \|\boldsymbol{y}_{\text{err}}(\ell)\|_{\boldsymbol{Q}}^2 + \lambda_u\|\Delta\boldsymbol{u}(\ell)\|_2^2$	Terminal cost ($\boldsymbol{R} \succ \boldsymbol{0}$)	[129]

With the objective function (7), the system model (5), and the explicit hard (input) and soft (state) constraints, the MPC problem that needs to be solved in real time takes the form

$$\begin{aligned} \underset{\boldsymbol{U}(k)}{\text{minimize}} \quad & J\big(\boldsymbol{x}(k), \boldsymbol{U}(k)\big) \\ \text{subject to} \quad & \boldsymbol{x}(\ell+1) = \boldsymbol{f}\big(\boldsymbol{x}(\ell), \boldsymbol{u}(\ell)\big) \\ & \boldsymbol{y}(\ell+1) = \boldsymbol{g}\big(\boldsymbol{x}(\ell+1)\big) \\ & \boldsymbol{u}(\ell) \in \boldsymbol{\mathcal{U}}_\epsilon \\ & \boldsymbol{x}(\ell+1) \in \boldsymbol{\mathcal{X}} \subseteq \mathbb{R}^{n_x} \\ & \forall\, \ell = k, \ldots, k+N_p-1\,. \end{aligned} \tag{8}$$

Depending on the nature of the optimization variable $\boldsymbol{U}(k)$ and the system (5), the optimization problem (8) is a generally hard-to-solve integer program (IP) [89], [135], or a usually easy-to-solve convex QP [136]. IPs, if computationally feasible, can be solved by exhaustively enumerating all candidate solutions. Alternatively, heuristics or dedicated optimization algorithms are required that decrease the *average* computational complexity, thus facilitating their real-time implementation without sacrificing optimality, see [26], [137], [138]. On the other hand, as mentioned before, convex optimization problems can be efficiently solved with off-the-shelf embedded solvers. A more detailed discussion on implementation issues of MPC is provided in Section IV.

C. Receding Horizon Policy

The solution to (8), i.e., the *optimal* sequence of manipulated variables

$$\boldsymbol{U}^*(k) = \Big[\boldsymbol{u}^{*T}(k) \quad \boldsymbol{u}^{*T}(k+1) \quad \ldots \quad \boldsymbol{u}^{*T}(k+N_p-1)\Big]^T, \tag{9}$$

is determined in an open-loop fashion. Therefore, applying $\boldsymbol{U}^*(k)$ to the system makes it susceptible to external disturbances, model inaccuracies, etc. To add feedback and provide the controller with a high degree of robustness, the notion of the receding horizon policy is employed, as shown in Fig. 3 for the direct MPC case. As can be seen, out of the sequence of optimal manipulated variables, only the first element $\boldsymbol{u}^*(k)$ is implemented. At the next time step, the optimization process is repeated over a one time-step shifted horizon based on new measurements and/or estimates, see Fig. 4.

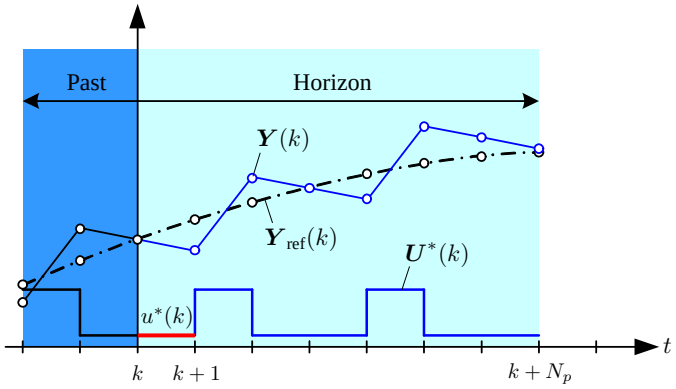

(a) Horizon at time step k

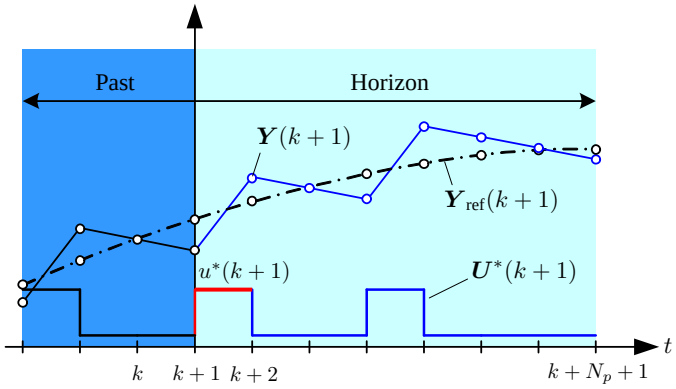

(b) Horizon at time step $k+1$

Fig. 3: Receding horizon policy of direct MPC for a single-input single-output (SISO) system. The predicted output and its reference trajectory are shown with $\boldsymbol{Y}(k) = [y(k+1) \ \ldots \ y(k+N_p)]^T$ and $\boldsymbol{Y}_{\text{ref}}(k) = [y_{\text{ref}}(k+1) \ \ldots \ y_{\text{ref}}(k+N_p)]^T$, respectively. A six-step prediction horizon ($N_p = 6$) is assumed.

III. Design Considerations

This section is dedicated to design considerations for MPC-based algorithms, either in their direct (Fig. 1(b)) or indirect (Fig. 1(a)) form. In the sequel, the most relevant design choices that affect the performance of such control schemes are discussed.

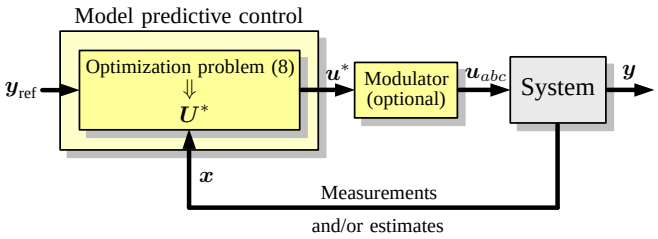

Fig. 4: Block diagram of MPC.

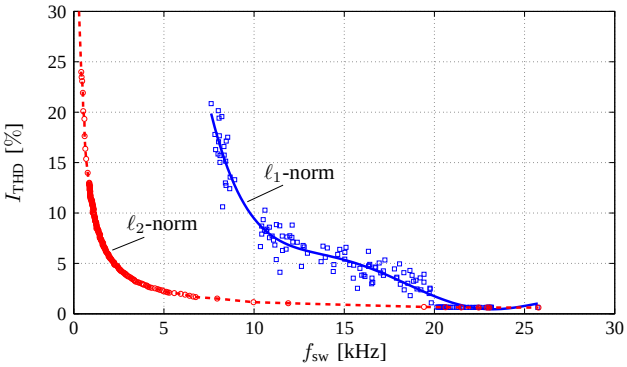

Fig. 5: Trade-off curves (taken from [33]) for direct MPC with reference tracking and the ℓ_1- or ℓ_2-norm. The current THD I_{THD} is shown for the achievable range of switching frequencies f_{sw}. The solid (blue) and dashed (red) lines are polynomial approximations of the individual simulation results indicated by squares (ℓ_1-norm) and circles (ℓ_2-norm), respectively. A system consisting of a two-level inverter and an induction machine is assumed.

A. Objective Function

As mentioned in Section II-B, and also shown in Table III, the kernel of the MPC problem, i.e., the objective function, can be designed in several ways and with different degrees of complexity. This great variety of choices employs the controller designer with degrees of freedom during the control formulation process, but it also affects the resulting performance. The first design choices one has to make relate to the norm used and the parameters included in the objective function.

1) Choice of Norm: When short-horizon direct MPC is employed, then a popular design choice is to use the ℓ_1-norm, see, e.g., [13], [21], [123], [126], [139], [140]. When the available computational power is of concern, such a choice is reasonable, since computation of the absolute values of the variable of concern is computationally cheap and straightforward. As shown in [141], however, ℓ_1-norm can lead to system performance deterioration and even stability issues, see Fig. 5.

In light of this, using the ℓ_2-norm with direct MPC is getting more popular, see, e.g., [26], [32], [120], [129], [142]–[144]. Another advantage of the ℓ_2-norm is that it turns the objective function into a quadratic one. When the optimization variable is a real-valued vector, then the solution to the unconstrained optimization problem can be easily found by setting the derivative of the objective function to zero [15]. This feature is utilized in direct MPC schemes that have an implicit modulator either when computing the application time of each switch position [52], [57], [60], [61], [63], or the online modifications of the offline computed switching patterns [79].

Regarding indirect MPC algorithms, the ℓ_2-norm is used in the vast majority—if not all—of the cases for the reasons mentioned above [101]–[103], [105]–[108]. Specifically, the formulated optimization problem based on the ℓ_2-norm is a QP which in its unconstrained version can be solved very easily since an analytical solution exists [105]–[108]. When input and/or state constraints exist, then either efficient QP solvers can be employed (see Section IV), or the unconstrained solution can be projected onto the feasible set [108].

2) Control Effort Penalization: According to the optimal control paradigm [1], [2], the control effort, modeled with the term $\Delta \boldsymbol{u}$ in Table III, is most commonly penalized in the objective function.[5] Depending on the type of MPC algorithm this has different interpretations, as explained below.

When direct MPC is concerned, penalization of the increment of the control signal in most cases implies direct control of the switching frequency [15].[6] In this context, lack of control effort penalization means that the *average* switching frequency f_{sw} is limited only by the chosen sampling frequency f_s, with $f_s = 1/T_s$. Specifically, the theoretical maximum switching frequency is equal to half the sampling frequency, i.e., $f_{\text{sw}} = f_s/2$, but in reality it is much lower than that [14, Chapter 4]. Moreover, as stated in [33], lack of penalization of the control effort leads to inferior system performance as compared to conventional control and modulation solutions, thus the potential of MPC is not fully exploited.

Regarding indirect MPC algorithms with a subsequent modulation stage, penalization of the control effort allows for less aggressive control actions and gives rise to smoother control [90], [99]. Moreover, given that $\lambda_u > 0$, where λ_u is the weighting factor of the control effort, the resulting QP is a strictly convex optimization problem [136], thus it guarantees the uniqueness of the solution [2].

B. Tuning Parameters

The main design parameters that affect the controller performance are the sampling interval T_s, the number of prediction horizon steps N_p and the several weighting factors, whether these relate to the controlled variables or the control effort. In the sequel, the most common tuning choices are presented.

1) Choice of Sampling Interval: The sampling interval not only affects the discretization accuracy and the ensuing stability of the discrete-time model, as mentioned in Section II-A, but also the controller performance. In direct MPC without implicit modulator switching can be performed only at the discrete time instants $kT_s, (k+1)T_s, \ldots$. Therefore, the aim is to have as high a sampling frequency as possible for a fine discretization of the time axis. To this end, sampling intervals of $150\,\mu$s or less are commonly chosen, see, e.g., [13], [23], [31], [127], [129], [144]–[147], with T_s being a few tens of microseconds with modern powerful control platforms, as discussed in Section IV. As mentioned in Section III-A2,

[5]Note that in other disciplines the manipulated variable $\boldsymbol{u}$ itself, rather than its rate of change $\Delta \boldsymbol{u}$, is frequently penalized [2].

[6]Exemption to that are some direct MPC algorithms with implicit modulator, e.g., MPC with programmed PWM, that achieve constant switching frequency [67], [79], [82].

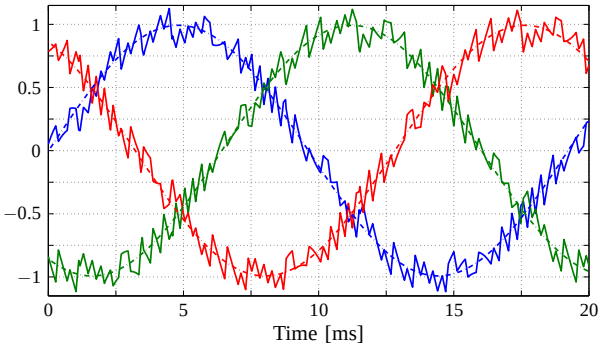

(a) Three-phase stator current $\boldsymbol{i}_{s,abc}$

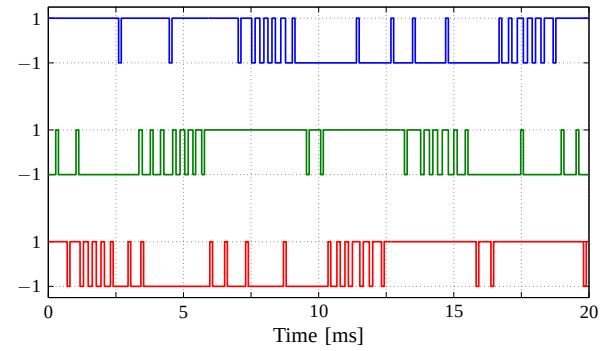

(b) Three-phase switch position $\boldsymbol{u}_{abc}$

Fig. 6: Direct MPC with output reference tracking. The sampling interval is $T_s = 25\,\mu$s ($f_s = 40$ kHz) and the switching frequency $f_{\text{sw}} \approx 1050$ Hz ($\lambda_u = 4.33 \cdot 10^{-3}$). A system consisting of a two-level inverter and an induction machine is assumed.

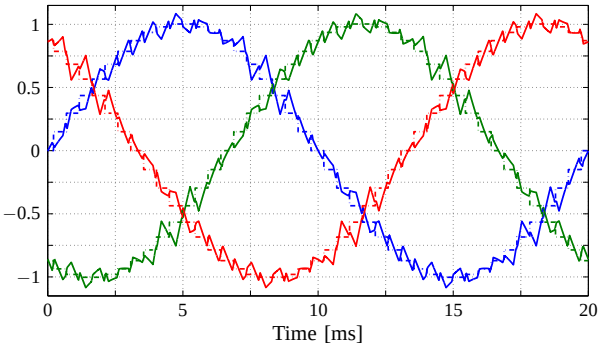

(a) Three-phase stator current $\boldsymbol{i}_{s,abc}$

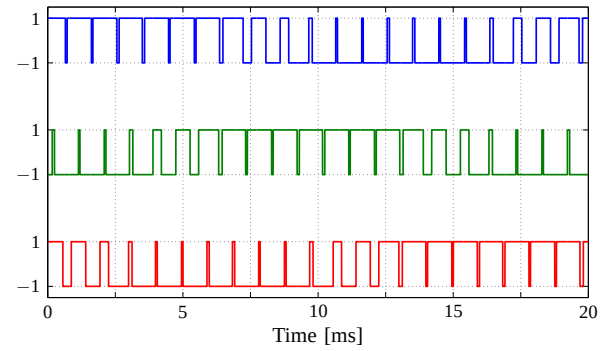

(b) Three-phase switch position $\boldsymbol{u}_{abc}$

Fig. 7: Indirect MPC with asymmetric regularly sampled SPWM. The sampling interval is $T_s \approx 476.19\,\mu$s ($f_s = 2100$ Hz) and the switching frequency $f_{\text{sw}} = 1050$ Hz. A system consisting of a two-level inverter and an induction machine is assumed.

this implies that the sampling frequency imposes an upper limit on the achievable switching frequency, which is most often adjusted by tuning the control effort weighting factor λ_u shown in Table III, see Fig. 6. It is worth mentioning, nonetheless, that as shown in [33], for a fine granularity of switching the ratio between the sampling and switching frequencies should be about 100.

On the other hand, direct MPC with implicit modulator can increase the granularity of switching by a factor of two or three, depending on whether two or three switch positions, respectively, are applied at the corresponding variable switching time instants within one sampling interval T_s [49], [50], [52], [54]–[58]. Moreover, when direct MPC with implicit modulator achieves operation at a fixed switching frequency then the latter is directly defined by the sampling interval due to the deterministic switching within one T_s [51], [53], [56], [59]–[61], [63], [65], [67], [68]. This implies that the sampling interval T_s defines the length of the fixed modulation cycle. For example, in case of two-level converters the relationship between the switching frequency f_{sw} and T_s is

$$f_{\text{sw}} = \frac{1}{2T_s}\,. \tag{10}$$

For direct MPC with programmed PWM, however, even though the switching frequency is constant—and as low as a few hundred Hz—it is decoupled from the sampling interval since such methods do not feature a modulation cycle of fixed length. In these methods, T_s is set as small possible—in the range of a few tens of microseconds—in order to avoid unnecessarily big deviations from the offline computed switching patterns as well as to provide the controller with a high degree of robustness to disturbances and system nonidealities [79], [80], [82], [83]. In doing so, both high-bandwidth controllers result and the applied switch positions manage to produce current harmonic distortions that are close to their minimum values.

Finally, similar to direct MPC with fixed switching frequency and modulation cycle, the sampling interval in indirect MPC with carrier-based PWM sets the operating switching frequency. When SVM or SPWM with asymmetric regular sampling are used then (10) holds for a two-level converter, i.e., the sampling frequency is twice the switching frequency [91], [94], [148], see Fig. 7. When, on the other hand, SPWM with symmetric regular sampling is used the sampling and switching frequency are the same if two-level converters are assumed [92], [97], [103], [105], [106].

2) Length of the Prediction Horizon: Long prediction horizons can improve the closed-loop system performance. Moreover, in case of infinite horizon, closed-loop stability is guaranteed if there exists a solution with a finite associated cost [1], [2]. Acknowledging such benefits, research effort has been put into the design and implementation of MPC algorithms with long horizons.

The benefits of direct MPC with long horizons have been discussed in, e.g., [33], [134]. Although the performance

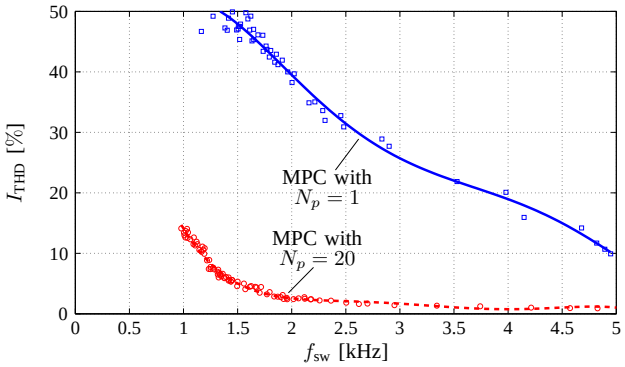

Fig. 8: Trade-off curves (taken from [33]) between stator current THD I_{THD} and switching frequency f_{sw} for direct MPC with output reference tracking for $N_p = 1$ (solid, blue line), and $N_p = 20$ (dashed, red line). The individual simulation results are shown with squares (MPC with $N_p = 1$), and circles (MPC with $N_p = 20$). A third-order system consisting of a two-level inverter, an LC filter and an induction machine is assumed. The resonance frequency is $f_{\text{res}} \approx 830\,\text{Hz}$.

improvement is indisputable—especially when higher-order systems are of concern, see Fig. 8—the challenge of long-horizon direct MPC relates to the implementation of the associated optimization problem. Specifically, as mentioned in Section II-B, in the vast majority of the cases the direct MPC problem is formulated as an IP which is NP-hard [89], meaning that its computational complexity increases exponentially with the number of candidate solutions. The latter depends on the topology in question and the length of the horizon. For example, assuming a three-phase two-level converter with input set

$$\mathcal{U}_\delta = \{-1, 1\}^3$$

then the possible solutions are 2^{3N_p}, while the elements of the optimization variable are $3N_p$. Hence, it can be understood that a longer horizon can render the direct MPC problem computationally intractable. In this sense, the approach of exhaustive enumeration is impractical with long-horizon direct MPC, thus one has to resort to other methods [137]. These include BnB strategies, such as the sphere decoder [26], [142], move blocking strategies [110], [127], event-based horizons [80], prediction with extrapolation or interpolation [39], [40], [48], or their combinations [42].

As for indirect MPC, long horizons improve the performance of such algorithms as well [99]. Similar to direct MPC, the optimization problem of explicit MPC is an IP—namely an (M)IQP—meaning that the same computational challenges exist. As a result, the implementation of long horizons can be demanding, thus the length of the horizon is limited to a few number of steps [90], [91], [94], [97]. MPC as a QP, however, allows for longer horizons owing to the convex nature of the problem, the implementation of which is easier with off-the-self solvers, as discussed in Section IV. Consequently, such MPC methods can achieve good closed-loop performance and avoid stability issues [5]. The same applies to direct MPC problems that can be formulated as QPs, as is the case of MPC with implicit modulator with either variable switching time instants [121] or programmed PWM [79], [81].

3) Tuning of the Weighting Factors: As can be observed in Table III, the objective functions may consist of more than one terms, giving rise to multi-criterion optimization problems. In such a case weighting factors are introduced to prioritize among the different, and probably conflicting, terms. Tuning of the associated weighting factors, i.e., λ_u (for the control effort) and the diagonal entries of $\boldsymbol{\Lambda}$ and $\boldsymbol{Q}$ (for the output terms), is not trivial [2].

In principle, the weighting factors in multi-criterion problems are found by exploring the trade-off curves or surfaces so as to find the Pareto optimal points [136, Section 4.7]. This, however, can be not only very time consuming and tedious, but also the trade-off curves can be nonconvex (i.e., neither monotonic nor smooth), as in the case of most direct MPC algorithms, see, e.g., Figs. 5 and 8. This means that choosing appropriate values for the weighting factors is even more challenging, motivating practitioners of MPC to resort to empirical approaches that rely on trial-and-error methods [149], [150].

To avoid heuristics, there have been some methods that choose the weighting factors based on analytical expressions, thus avoiding tuning altogether [115], [151], [152]. Moreover, emerging methods for the weighting factors tuning utilize techniques from artificial intelligence, such as neural networks and genetic algorithms [143], [153]–[155]. In this way the tuning process is automated and the weighting factors can be adjusted in real time. The downside of the former methods, however, is that their generalization and applicability to different power electronic systems are limited, whereas the latter require elaborate design process and the training procedure can be very laborious and non-exhaustive.

C. Robustness

As discussed in Section II-A, MPC requires an accurate system model to achieve favorable performance. Even though the models of power electronic systems are typically accurate—at least compared to other disciplines—model mismatches and system nonidealities are always present, due to, e.g., component aging, temperature variations, etc. Such inaccuracies can adversely affect the system performance [156]. Such performance deterioration is also amplified by the lack of an integrating element from MPC that facilitates the elimination of steady-state errors. Despite the fact that the receding horizon makes the MPC schemes robust to disturbances, model uncertainties and mismatches, further tools and methods are required to ensure smooth operation of the power electronic system.

For addressing the lack of integrating action of MPC and the ensuing steady-state errors due to model mismatches, etc., some techniques have been proposed that add an explicit integrator either to the objective fucntion [157], [158], or to the state vector [92]. Alternatively, disturbance observers, such as integral feedback observers, Luenberger observers, (extended) Kalman filters, moving horizon estimation, can be implemented to add an integrating action to the outer loop [103], [110], [159]–[161]. Moreover, system identification algorithms can be employed that either assume knowledge of the system (i.e., white-box model-based approaches) [162]–[164], or are model free (i.e., black box methods) [165]–[168].

Note, however, that the former methods fail to estimate all the system parameters at once, while combinations of different sources of uncertainties/model mismatches are usually neglected, implying that the estimation performance is not the most desired. As for the latter, they rely on measurements of the input and output signals (e.g., applied voltage and load current, respectively) and elaborate look-up tables, which are subsequently utilized by computational demanding identification techniques, such as data fitting methods. As a result, the already pronounced computational load of MPC is further increased.

D. Stability

MPC is a time-domain nonlinear control technique. Thus, traditional frequency-domain stability analysis tools are not applicable. Moreover, depending on the system modeling and the subsequent control problem formulation, MPC deals with plants with integer inputs. Stability of such systems is intrinsically difficult to study and prove.

For the study of closed-loop stability of indirect MPC Lyapunov stability theory is employed [169]. More specifically, first, the designer has to define an invariant set $\boldsymbol{X}_f$ under a terminal control law of the form $\nu(\star)$ applied after the horizon N_p. Following, a Lyapunov function in $\boldsymbol{X}_f$ is included in the objective function in the form of a terminal cost, see, e.g., function J_{11} in Table III. Moreover, the state constraints in problem (8) need to be augmented by a terminal constraint $\boldsymbol{x}(k+N_p) \in \boldsymbol{X}_f$ [170], [171]. In doing so, indirect MPC schemes with carrier-based PWM—either formulated as QP [111] or (M)IQP which employs explicit MPC [92], [172], [173]—that guarantee closed-loop stability can be designed.

Regarding direct MPC, closed-loop (practical) asymptotic stability was shown in [174], [175], assuming power electronic systems that can be modeled as linear systems with integer inputs.[7] To achieve this, similarly to indirect MPC, a Lyapunov-based stabilizing quadratic objective function needs to be designed. Based on these works, [141] showed that direct MPC based on the ℓ_1-norm can lead to instability provided that the control effort is penalized (see, function J_6 in Table III). On the other hand, when $\lambda_u = 0$ (see, e.g., J_2 or J_4 in Table III) then potential stability issues are avoided, as also verified in [176], [177]. Moreover, closed-loop stability of one-step direct MPC was achieved in [178] by introducing constraints that ensure the asymptotic convergence of the controlled variables. Furthermore, an interesting approach for the verification of the behavior of direct MPC for different power electronic was proposed in [179]. By employing tools from statistics, this work aims to take the relevant research one step further than [174], [175]. Due to the nature of the adopted tools (i.e., statistical model checking), however, this method is not deterministic and lacks rigorous mathematical exactitude. Finally, practical stability of systems governed by direct MPC with hysteresis bounds as well as conditions to ensure operation within a safe region were provided in [180]. To do so, as with the above-mentioned works, Lyapunov stability theory was utilized to tackle the problem at hand.

[7]The definition and implications of closed-loop practical stability are provided in [174, Section II] and references therein.

IV. Implementation

Power electronic systems require sampling frequencies of a few up to several tens of kHz due the very small time constants that characterize them. For this reason the real-time implementation of control schemes in the framework of MPC is not trivial. Specifically, solving in real time the underlying integer QP (IQP) or QP within the available time of a few microseconds poses the main challenge.

In this section implementation-related issues of both direct and indirect MPC are discussed. Available options on how to solve the associated optimization problems in real time are presented. Moreover, considering the computational complexity of most MPC algorithms, powerful control platforms are often needed to fully utilize the available computational power. To this end, this section also offers options based on system-on-chip (SoC) technology with digital signal processors (DSPs) or field-programmable gate arrays (FPGAs) and ARM processors.

A. Solvers

As mentioned, direct MPC for power electronics is most often formulated as an IQP. The common practice for solving such optimization problems in embedded control systems is with exhaustive search. Since the problem is NP-hard, such an approach is impractical for horizons longer than one step ($N_p > 1$), see Section III-B2. Hence, as discussed in that section, more sophisticated algorithms are necessary to realize longer horizons at high sampling frequencies.

From an implementation point of view, a method that has attracted particular attention in recent years is a BnB algorithm named sphere decoder [26] thanks to its ostensible effectiveness; the average computational burden of sphere decoder scales linearly (instead of exponentially) with the prediction horizon steps [181]. As a result, this solver has been implemented in [144], [146], [147], [182], for different power electronics applications. In [146], a three-step ($N_p = 3$) direct MPC for a five-level converter was implemented with a sampling frequency $f_s = 10\,\text{kHz}$ ($T_s = 100\,\mu\text{s}$). A four-step horizon ($N_p = 4$) for a three-level converter was implemented in [147], but with the slightly higher sampling interval $T_s = 125\,\mu\text{s}$. A four-step horizon was also implemented in [144] with $T_s = 25\,\mu\text{s}$ for a two-level converter. All the three previous works used a dSpace system as control platform. The first FPGA-based implementation was presented in [182]. Therein, a horizon of $N_p = 5$ time steps was achieved for a three-level converter, while the sampling interval was set to $T_s = 25\,\mu\text{s}$.

An alternative approach to solve the IQP underlying direct MPC in an efficient manner is to adopt the so-called miOSQP solver [183] which is based on the alternating direction method of multipliers (ADMM) [184]. This algorithm was employed in [129] to solve the direct MPC problem for a three-level converter. As shown, short horizons suffice to achieve favorable system performance when a terminal cost—intended to

TABLE IV: Summary of solvers used in MPC for power electronics

Solver	Method	Problem	Matlab interface	Open source
qpOASES	AS	QP	yes	yes
ODYS	IP	QP	no	no
Sphere decoder	BnB	IQP	no	no
miOSQP	ADMM	IQP	no	yes

approximate an infinite horizon cost—is added to the objective function. This was verified with results acquired based on an FPGA implementation for $N_p = 2$ and $T_s = 25\,\mu$s.

Regarding MPC problems formulated as QPs (e.g., indirect MPC with carrier-based PWM, or some direct MPC algorithms with implicit modulator, such as MPC with programmed PWM), they can be solved with any of the available (both open-source and commercial) QP solvers. These options differ in their approach in solving the optimization problem. Several algorithms have been proposed in literature, such as interior-point (IP), active-set (AS), gradient, and explicit methods, as well as the aforementioned ADMM. A comprehensive assessment of different QP solvers is given in [185] and, with more focus on FPGA implementation, in [186]. Besides numerical accuracy, the computational speed of the solver is crucial. It is important to note that the relevant quantity is the worst-case execution time as this determines the maximum sampling frequency. The execution time depends on many factors, such as the size of the state and input vectors, number of constraints, steps of the horizon as well as the type of calculation unit used. Another aspect when choosing a solver is which interfaces are offered. For the power electronics domain, an interface to software such as Matlab/Simulink would be the favored choice, as it allows simple integration into closed-loop simulations.

A solver that has been gaining popularity in the power electronics community is qpOASES [187]. This solver was employed in [101] to solve a linear QP underlying indirect MPC for a motor drive system in less than $100\,\mu$s. Moreover, this solver was used in combination with the ACADO [188] and casADi [189] toolkits in [103] and [100], respectively, again for electrical drives. In all the above works the solver was implemented on a dSpace system. Another advantage of qpOASES is that it is suitable for nonlinear QPs owing to available abstraction tools that tailor the solver to the QP at hand and generate an optimized code that can also take the processor architecture into account, see, e.g., [190]–[192]. Finally, ODYS, a QP solver with low computational and memory requirements that employs an AS method, showed promising results with a drive system [102].

Given the above, Table IV summarizes some key aspects about solvers that have been used with a telling effect in MPC for power electronics.

B. Systems

One of the main challenges in implementing MPC algorithms is handling the potentially high computational burden within the small sampling intervals. This leads to the question of a suitable embedded calculation platform. The list of candidates includes DSPs, FPGAs, micro-controller units (MCUs), and their combinations. Typically, an embedded control system for power electronics includes an FPGA to manage the inputs and outputs (IOs) of the system, such as generation of the gate signals and the reading values from the analog-to-digital converters (ADCs). In conjunction with the FPGA, often one or more MCUs or DSPs are added to calculate the entire (or a part) of the control algorithm and realize interfaces to other systems.

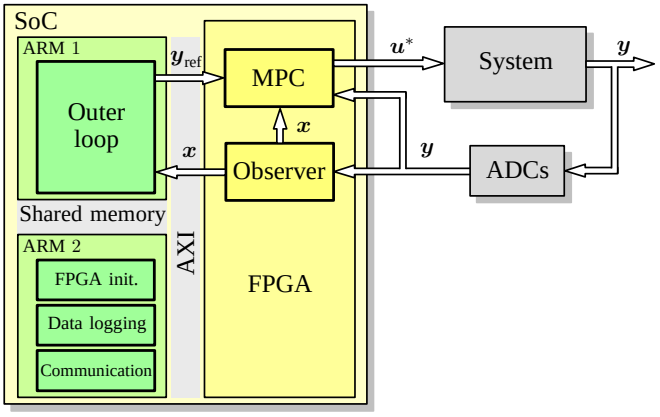

Fig. 9: FPGA-based SoC structure for the implementation of direct MPC.

Due to the fact that most direct MPC algorithms require a sampling frequency of about two orders of magnitude higher than the desired switching frequency [33], FPGAs are the most promising control platform owing to their ability to perform calculations in a highly pipelined and parallelized manner [129], [182]. For example, direct MPC with horizon $N_p = 2$ and sampling interval $T_s = 10\,\mu$s ($f_s = 100\,$kHz) was solved with exhaustive search on an FPGA by pipelining all possible predictions [193].

One drawback of these multi-chip solutions is the possible communication bottleneck between the FPGA and the other calculation units. An FPGA-based SoC overcomes this issue by combining the FPGA and multiple processor cores in one silicon chip. The calculation units are highly interconnected by the standardized advanced extensible interface (AXI) which provides an on-chip, high bandwidth, low latency interface between the processing system (PS) and the programmable logic (PL). This allows to leverage the advantages of an FPGA in multiple ways, namely, the FPGA can be used for the calculation of all the control-associated procedures and by this closing the control loop directly in the PL. Another option is to use the FPGA as an accelerator for the processor and use the PS for operations that can be done more efficiently there, e.g., divisions, or matrix inversions. Following, parallelizable computations can be offloaded to the FPGA. In recent years, several research groups have built their own control platforms based on FPGA SoCs, see, e.g., [193]–[198].

Fig. 9 depicts a simplified example of the implementation of direct MPC on an SoC FPGA. First, the measurements are read from the ADCs and processed by an optional observer to get the current state $\boldsymbol{x}(k)$.[8] Subsequently, the MPC algorithm

[8]To simplify the diagram, the delay compensation is omitted.

TABLE V: Assessment of direct MPC schemes. "MPC w. ref. track." stands for MPC with reference tracking (i.e., FCS-MPC), "MPC w. hyst. bounds" for MPC with hysteresis bounds, "MPC w. var. sw. inst." for MPC with variable switching time instants, and "MPC w. prog. PWM" for MPC with programmed PWM. Only the relevant objective functions for each MPC scheme are indicated.

Objective function (Table III)	Direct MPC scheme	Design complexity	Computational complexity	Performance	Stability
$J_1 = \|\boldsymbol{u}(k) - \boldsymbol{u}(k-1)\|_1$	MPC w. hyst. bounds	Simple	Low	Good	Stable
$J_2 = \|\boldsymbol{y}_{\text{err}}(k+1)\|_1$	MPC w. ref. track.	Simple	Low	Poor	Stable
	MPC w. var. sw. inst.	Simple	Moderate	Poor	Stable
$J_3 = \|\boldsymbol{y}_{\text{err}}(k+1)\|_2^2$	MPC w. ref. track.	Simple	Moderate	Poor	Stable
	MPC w. var. sw. inst.	Simple	Moderate	Good	Stable
	MPC w. prog. PWM	Moderate	Low	Very good	Stable
$J_4 = \|\boldsymbol{\Lambda}\boldsymbol{y}_{\text{err}}(k+1)\|_1$	MPC w. ref. track.	Complex	Low	Poor	Stable
	MPC w. var. sw. inst.	Complex	Moderate	Poor	Stable
$J_5 = \|\boldsymbol{y}_{\text{err}}(k+1)\|_{\boldsymbol{Q}}^2$	MPC w. ref. track.	Complex	Moderate	Poor	Stable
	MPC w. var. sw. inst.	Complex	Moderate	Good	Stable
	MPC w. prog. PWM	Complex	Low	Very good	Stable
$J_6 = \|\boldsymbol{y}_{\text{err}}(k+1)\|_1 + \lambda_u\|\Delta\boldsymbol{u}(k)\|_1$	MPC w. ref. track.	Moderate	Low	Poor	Potentially unstable
	MPC w. var. sw. inst.	Complex	Moderate	Poor	Potentially unstable
$J_7 = \|\boldsymbol{y}_{\text{err}}(k+1)\|_2^2 + \lambda_u\|\Delta\boldsymbol{u}(k)\|_2^2$	MPC w. ref. track.	Moderate	Moderate	Very good	Stable
	MPC w. var. sw. inst.	Complex	Moderate	Very good	Stable
	MPC w. prog. PWM	Complex	Low	Excellent	Stable
$J_8 = \sum_{\ell=k}^{k+N_p-1} \|\Delta\boldsymbol{u}(\ell)\|_1$	MPC w. hyst. bounds	Moderate	Moderate	Excellent	Stable
$J_9 = \sum_{\ell=k}^{k+N_p-1} \|\boldsymbol{y}_{\text{err}}(\ell+1)\|_2^2 + \lambda_u\|\Delta\boldsymbol{u}(\ell)\|_2^2$	MPC w. ref. track.	Complex	High	Excellent	Stable
	MPC w. var. sw. inst.	Complex	Moderate/High	Very good	Stable
	MPC w. prog. PWM	Complex	Moderate	Excellent	Stable
$J_{10} = \sum_{\ell=k}^{k+N_p-1} \|\boldsymbol{y}_{\text{err}}(\ell+1)\|_{\boldsymbol{Q}}^2 + \lambda_u\|\Delta\boldsymbol{u}(\ell)\|_2^2$	MPC w. ref. track.	Complex	High	Excellent	Stable
	MPC w. var. sw. inst.	Complex	Moderate/High	Very good	Stable
	MPC w. prog. PWM	Complex	Moderate	Excellent	Stable
$J_{11} = \|\boldsymbol{y}_{\text{err}}(k+N_p)\|_{\boldsymbol{R}}^2 + \sum_{\ell=k}^{k+N_p-1} \|\boldsymbol{y}_{\text{err}}(\ell)\|_{\boldsymbol{Q}}^2 + \lambda_u\|\Delta\boldsymbol{u}(\ell)\|_2^2$	MPC w. ref. track.	Complex	High	Excellent	Stable
	MPC w. var. sw. inst.	Complex	Moderate/High	Very good	Stable
	MPC w. prog. PWM	Complex	Moderate	Excellent	Stable

TABLE VI: Assessment of indirect MPC schemes. Only the relevant objective functions for each MPC scheme are indicated.

Objective function (Table III)	Indirect MPC scheme	Design complexity	Computational complexity	Performance	Stability
$J_3 = \|\boldsymbol{y}_{\text{err}}(k+1)\|_2^2$	MPC as (M)IQP	Simple	Moderate	Good	Stable
	MPC as QP	Simple	Low	Good	Stable
$J_5 = \|\boldsymbol{y}_{\text{err}}(k+1)\|_{\boldsymbol{Q}}^2$	MPC as (M)IQP	Complex	Moderate	Good	Stable
	MPC as QP	Complex	Low	Good	Stable
$J_7 = \|\boldsymbol{y}_{\text{err}}(k+1)\|_2^2 + \lambda_u\|\Delta\boldsymbol{u}(k)\|_2^2$	MPC as (M)IQP	Moderate	Moderate	Very good	Stable
	MPC as QP	Moderate	Low	Very good	Stable
$J_9 = \sum_{\ell=k}^{k+N_p-1} \|\boldsymbol{y}_{\text{err}}(\ell+1)\|_2^2 + \lambda_u\|\Delta\boldsymbol{u}(\ell)\|_2^2$	MPC as (M)IQP	Complex	High	Very good	Stable
	MPC as QP	Moderate	Moderate	Very good	Stable
$J_{10} = \sum_{\ell=k}^{k+N_p-1} \|\boldsymbol{y}_{\text{err}}(\ell+1)\|_{\boldsymbol{Q}}^2 + \lambda_u\|\Delta\boldsymbol{u}(\ell)\|_2^2$	MPC as (M)IQP	Complex	High	Very good	Stable
	MPC as QP	Complex	Moderate	Very good	Stable
$J_{11} = \|\boldsymbol{y}_{\text{err}}(k+N_p)\|_{\boldsymbol{R}}^2 + \sum_{\ell=k}^{k+N_p-1} \|\boldsymbol{y}_{\text{err}}(\ell)\|_{\boldsymbol{Q}}^2 + \lambda_u\|\Delta\boldsymbol{u}(\ell)\|_2^2$	MPC as (M)IQP	Complex	High	Very good	Stable
	MPC as QP	Complex	Moderate	Very good	Stable

is executed in the FPGA. The reference $\boldsymbol{y}_{\text{ref}}(k)$ is provided by an outer control loop, which runs at a lower frequency on the ARM processor 1. The interface between the control loops is realized by the integrated AXI. The other depicted ARM processor is not part of the control loop and attends "housekeeping" tasks, such as the initialization of the FPGA, data logging and communication with the other systems and the user.

In addition to embedded control systems, commercial rapid-control-prototyping (RCP) systems have been used in combination with the solvers discussed in Section IV-A for the experimental validation of indirect MPC algorithms. Such systems include the aforementioned dSpace, and the realized sampling frequencies are in the order of $10\,\text{kHz}$ [101], [103], [192]. In addition indirect MPC has also been implemented using OPAL RT, which combines multi-core CPUs linked to an

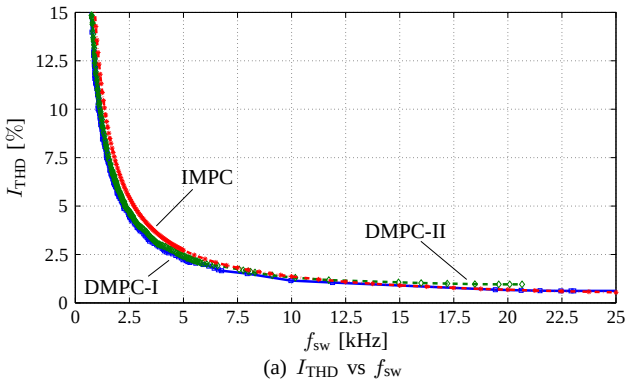

(a) I_{THD} vs f_{sw}

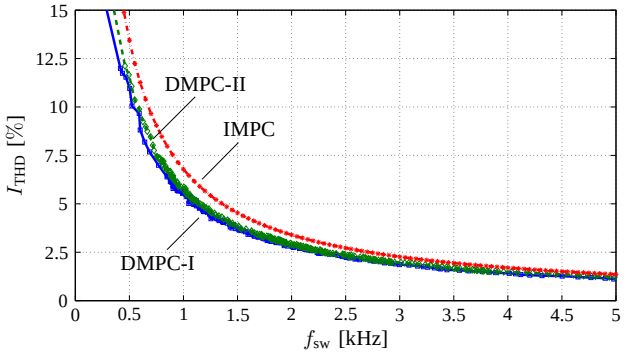

(b) I_{THD} vs f_{sw} (zoomed in)

Fig. 10: Trade-off between current THD I_{THD} and switching frequency f_{sw} for direct MPC with output reference tracking (DMPC-I; shown with a solid, blue line), direct MPC with variable switching time instants (DMPC-II; shown with a dashed, green line), and indirect MPC with SVM (IMPC; shown with a dash-dotted, red line). The individual simulations are shown as squares (DMPC-I), rhombi (DMPC-II), and asterisks (IMPC). A system consisting of a two-level inverter and an induction machine is assumed.

FPGA, see [199], or even low-cost DSP-based platforms [102].

V. Assessment

In this section a brief assessment of MPC methods for power electronics is provided. First, Tables V and VI present a qualitative evaluation of the discussed direct and indirect MPC algorithms, respectively, in terms of design and computational complexity, resulting system performance and closed-loop stability. This is done for the different objective functions presented in Table III. The aim of Tables V and VI is to indicate in a concise manner the associated potential, challenges and pitfalls of the different formulations of the MPC problem. As can be seen, MPC, both in its direct and indirect versions, achieves the best performance when long horizons are implemented. This, however, comes at a cost of increased computational and design complexity, implying that MPC algorithms most often require powerful control platforms to be realized in a real-world setup, see Section IV-B. Hence, MPC is mostly relevant for applications where the cost of such platforms is negligible—or, at least, low—when compared to the cost of the power electronic system in question, and—more importantly—to the associated cost savings achieved due to the performance improvement accredited to MPC.

Fig. 10 presents a comparison between direct MPC with reference tracking ($N_p = 1$, $T_s = 5\,\mu$s), direct MPC with implicit modulator and one variable switching time instant ($N_p = 1$, $T_s = 10\,\mu$s) [200], and indirect MPC with SVM ($N_p = 1$, T_s chosen according to (10)) in terms of stator current THD over a wide range of switching frequencies. The objective function used in all cases is J_7 from Table III. The case study relates to an electrical drive system consisting of a two-level inverter and an induction machine; the parameters of the system are given in [33, Appendix A]. As can be observed, direct MPC, regardless of its implementation, outperforms indirect MPC with SVM as the switching frequency decreases. The reason is that switching with indirect MPC is deterministic and constrained by the dedicated modulator, whereas direct MPC has the freedom to make decisions and apply a new switch position at a much higher frequency rate.

However, although Fig. 10 indicates the superiority of direct MPC—in terms of current THD—for drive systems, indirect MPC is an excellent option for grid-connected converters. Direct MPC—with the exemption of some direct MPC schemes with implicit modulator, such as programmed PWM—due to the lack of a modulator produces switching patterns that are not repetitive. This implies that the harmonic spectra are nondeterministic, with the harmonic energy spread over the whole range of frequencies. A direct consequence of this is that grid standards, such as the IEEE 519 [201], cannot be met since they impose stringent limits on harmonics at the point of common coupling (PCC), especially of even order and interharmonics.

To further explain why direct—as opposed to indirect—MPC may not be suitable for grid-tied converters an example is provided hereafter. Consider a grid-tied two-level converter with an LCL filter with resonance frequency $f_{\text{res}} = 1203.3$ Hz and direct MPC with reference tracking with a three-step prediction horizon ($N_p = 3$) and sampling interval $T_s = 40\,\mu$s. For a switching frequency of about 2850 Hz, the output current spectrum is shown in Fig. 11(a). In addition, Fig. 11(b) depicts the harmonics of non-integer order lumped together to the closest integer harmonic by computing an equivalent rms value along with the harmonic limits imposed by the standard. By doing so, a direct comparison with the limits imposed by the IEEE 519 standard can be performed. Specifically, the standard limits are shown as light gray bars, harmonics that meet these limits are shown as blue bars, and harmonics violating their limits as red bars. As can be seen, although the odd harmonics can meet the limits, harmonics of even order within the range 10 to 25 violate—even marginally—their limits. For example, the 12^{th} harmonic has amplitude $0.91\,\%$ which is greater than the $0.875\,\%$ limit of the standard.

Moreover, it can be observed that the harmonic energy is not concentrated around the switching frequency, i.e., 2850 Hz, but it is spread over low-order harmonics. This is because harmonics beyond the resonance frequency (here 1203.3 Hz) are effectively attenuated, whereas low-frequency harmonics are not. As a result, all these low-order harmonics are not filtered out but appear in the spectrum. Such a characteristic renders direct MPC unsuitable for grid-tied converters, unless long horizons are used to drastically reduce the harmonic distortions, see Fig. 8 and [33].

On the other hand, owing to the deterministic spectrum of

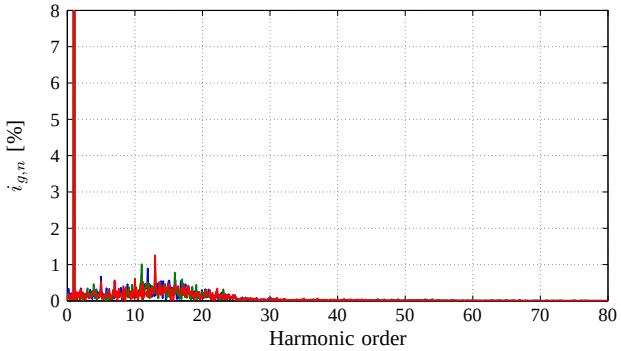

(a) Current harmonic spectrum for switching frequency $f_{\text{sw}} \approx 2850\,\text{Hz}$.

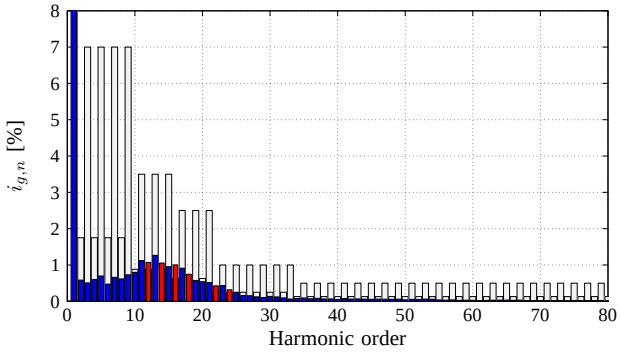

(b) Current harmonic spectrum with respective harmonic limits at the PCC based on the IEEE 519 standard for a short-circuit ratio of $k_{\text{sc}} = 20$.

Fig. 11: Current harmonic spectrum produced by direct MPC.

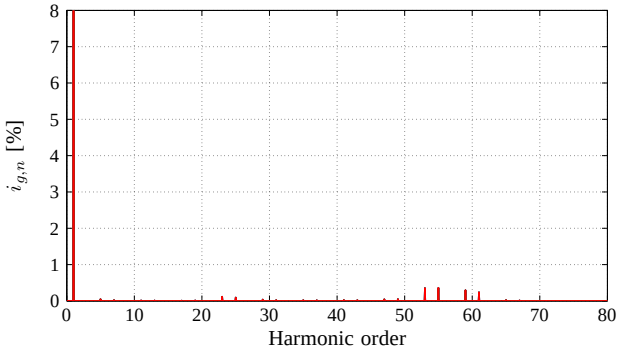

(a) Current harmonic spectrum for switching frequency $f_{\text{sw}} = 2850\,\text{Hz}$.

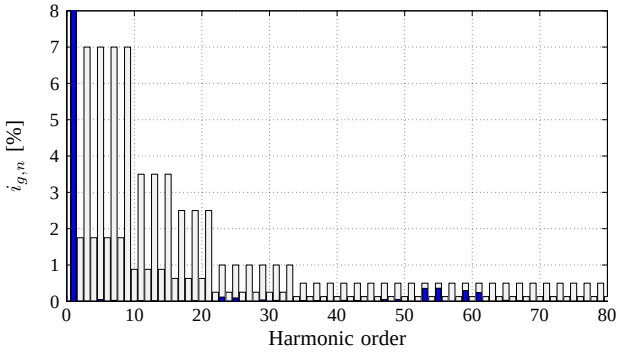

(b) Current harmonic spectrum with respective harmonic limits at the PCC based on the IEEE 519 standard for a short-circuit ratio of $k_{\text{sc}} = 20$.

Fig. 12: Current harmonic spectrum produced by indirect MPC.

PWM, the harmonic energy of the grid current with indirect MPC is concentrated at the sideband harmonics, see Fig. 12. Hence, low-frequency harmonics are of very small amplitude, whereas harmonics at frequencies higher than the resonance are effectively filtered out.

VI. Trends

The last part of this survey provides the current trends and contemporary aspects of MPC in academia and industry.

As highlighted in Section III-B1, the sampling interval for direct MPC needs to be as low as possible to achieve a fine granularity of switching. Because of this, the research interest moves towards control platforms that can enable the implementation of MPC algorithms with very high sampling frequencies—see also Section IV-B—as well as algorithms that can keep the computational complexity of MPC at bay.

The latter is a very relevant research question from an industrial point of view as well. Specifically, one of the main industrial research focuses is on techniques that mitigate the pronounced computational complexity [202]. Such methods will facilitate the real-time implementation of refined MPC algorithms and, as a result, their potential will be utilized to its full extent. In doing so, MPC will be able to bring palpable benefits to the industry, such as reduction of the investment or operating costs of the power electronic system [202], thus establishing it as a superior control alternative to the conventional solutions. It is worth mentioning that the existing MPC-based industrial control solutions support the above argument [79], [190].

Another emerging research direction relates to the formulation of the MPC problem. Many of the derived MPC algorithms and/or solvers assume linear systems of the form (4) with integer or real-valued inputs, see, e.g., [26], [105]. Given that many power electronic systems do not meet such a prerequisite, this means that they either have to be linearized [99], [203], thus detracting from the accuracy of the model, or other methods need to be developed and/or solvers employed. To tackle these issues, MPC needs to be addressed as a nonlinear problem [204]. Moreover, solvers, such as the aforementioned qpOASES [187], FORCES [205], etc., and toolkits, e.g., ACADO [188], casADi [189], VIATOC [206], etc., can be adopted for indirect MPC. As for direct MPC, either existing methods, such as the sphere decoder [26], need to be extended to nonlinear systems and the optimization problem to be reformulated [207], or new algorithms need to be developed.

Finally, an interesting topic is the development of MPC algorithms that achieve both low harmonic distortions with discrete harmonic spectra as well as excellent dynamic behavior. As highlighted in Section V, indirect MPC with carrier-based PWM can produce spectra with harmonics appearing at odd non-triplen multiples of the fundamental frequency. Moreover, it can potentially achieve very low THD (e.g., when LC or LCL filters are present). However, its dynamic behavior is worse than that of direct MPC due to the existence of the explicit modulator. Therefore, combining principles from both direct and indirect MPC is apropos. To this aim, direct MPC with implicit modulator, either in the form of programmed PWM [79], [208], [209], or variable switching

time instants [67], [121], seems as a very promising direction.

VII. Conclusions

MPC, either with modulator (i.e., indirect MPC) or without (i.e., direct MPC), has been an emerging control method in the field of power electronics. In this survey, the formulation of the optimization problem underlying MPC has been discussed along with the most relevant design considerations and the associated controller robustness and closed-loop system stability. A properly designed objective function is vital to avoid stability issues, while tuning parameters, such as the sampling interval, the length of the horizon and the weighting factors (when present) profoundly affect the performance of the controller. Based on the presented assessment of the most common MPC methods, it can be concluded that MPC, when properly designed for and tailored to a given case study, can achieve favorable system performance. This, however, comes at the expense of pronounced computational complexity—especially when implemented naively—implying that powerful control platforms and efficient real-time solvers are required in many cases. To this end, the most up-to-date systems and solvers have been identified and their potential and applicability presented. Nevertheless, despite the existing solutions further research is required to fully utilize the potential of MPC. For this reason, future meaningful directions have been pinpointed aiming to motivate current and future practitioners of MPC in the field of power electronics.

References

[1] E. F. Camacho and C. Bordons, *Model predictive control*. London, UK: Springer-Verlag, 2007.

[2] J. B. Rawlings and D. Q. Mayne, *Model predictive control: Theory and design*. Madison, WI, USA: Nob Hill, 2009.

[3] J. Richalet, A. Rault, J. L. Testud, and J. Papon, "Model predictive heuristic control: Applications to industrial processes," *Automatica*, vol. 14, no. 5, pp. 413–428, Sep. 1978.

[4] C. R. Cutler and B. L. Ramaker, "Dynamic matrix control—A computer control algorithm," in *Proc. Nat. Meet. of the Amer. Instit. of Chemical Eng.*, Houston, TX, USA, Apr. 1979.

[5] M. Morari and J. H. Lee, "Model predictive control: Past, present and future," *Comput. and Chemical Eng.*, vol. 23, no. 4–5, pp. 667–682, May 1999.

[6] D. Q. Mayne, "Model predictive control: Recent developments and future promise," *Automatica*, vol. 50, no. 12, pp. 2967–2986, Dec. 2014.

[7] S. J. Qin and T. A. Badgwell, "A survey of industrial model predictive control technology," *Control Eng. Pract.*, vol. 11, no. 7, pp. 733–764, Jul. 2003.

[8] J. Holtz and S. Stadtfeld, "A predictive controller for the stator current vector of ac-machines fed from a switched voltage source," in *Proc. Int. Power Electron. Conf.*, Tokyo, Japan, Mar. 1983, pp. 1665–1675.

[9] D. F. Schröder and R. Kennel, "Model-control PROMC—A new control strategy with microcomputer for drive applications," *IEEE Trans. Ind. Appl.*, vol. IA-21, no. 5, pp. 1162–1167, Sep./Oct. 1985.

[10] R. Kennel, A. Linder, and M. Linke, "Generalized predictive control (GPC)–Ready for use in drive applications?" in *Proc. IEEE Power Electron. Spec. Conf.*, Vancouver, BC, Canada, Jun. 2001, pp. 1839–1844.

[11] A. Linder and R. Kennel, "Model predictive control for electrical drives," in *Proc. IEEE Power Electron. Spec. Conf.*, Recife, Brazil, Jun. 2005, pp. 1793–1799.

[12] T. Geyer, G. Papafotiou, and M. Morari, "On the optimal control of switch-mode dc-dc converters," in *Hybrid Syst.: Comput. and Control*, ser. LNCS, R. Alur and G. J. Pappas, Eds. Berlin, Germany: Springer-Verlag, 2004, vol. 2993, pp. 342–356.

[13] J. Rodríguez, J. Pontt, C. A. Silva, P. Correa, P. Lezana, P. Cortés, and U. Ammann, "Predictive current control of a voltage source inverter," *IEEE Trans. Ind. Electron.*, vol. 54, no. 1, pp. 495–503, Feb. 2007.

[14] J. Rodríguez and P. Cortés, *Predictive control of power converters and electrical drives*. Chichester, UK: Wiley, 2012.

[15] T. Geyer, *Model predictive control of high power converters and industrial drives*. Hoboken, NJ, USA: Wiley, 2016.

[16] P. Cortés, M. P. Kazmierkowski, R. M. Kennel, D. E. Quevedo, and J. Rodríguez, "Predictive control in power electronics and drives," *IEEE Trans. Ind. Electron.*, vol. 55, no. 12, pp. 4312–4324, Dec. 2008.

[17] S. Kouro, P. Cortés, R. Vargas, U. Ammann, and J. Rodríguez, "Model predictive control—A simple and powerful method to control power converters," *IEEE Trans. Ind. Electron.*, vol. 56, no. 6, pp. 1826–1838, Jun. 2009.

[18] J. Rodríguez, M. P. Kazmierkowski, J. R. Espinoza, P. Zanchetta, H. Abu-Rub, H. A. Young, and C. A. Rojas, "State of the art of finite control set model predictive control in power electronics," *IEEE Trans. Ind. Informat.*, vol. 9, no. 2, pp. 1003–1016, May 2013.

[19] S. Kouro, M. A. Perez, J. Rodríguez, A. M. Llor, and H. A. Young, "Model predictive control: MPC's role in the evolution of power electronics," *IEEE Ind. Electron. Mag.*, vol. 9, no. 4, pp. 8–21, Dec. 2015.

[20] S. Vazquez, J. Rodríguez, M. Rivera, L. G. Franquelo, and M. Norambuena, "Model predictive control for power converters and drives: Advances and trends," *IEEE Trans. Ind. Electron.*, vol. 64, no. 2, pp. 935–947, Feb. 2017.

[21] R. Vargas, P. Cortés, U. Ammann, J. Rodríguez, and J. Pontt, "Predictive control of a three-phase neutral-point-clamped inverter," *IEEE Trans. Power Electron.*, vol. 24, no. 5, pp. 2697–2705, Oct. 2007.

[22] P. Cortés, J. Rodríguez, P. Antoniewicz, and M. Kazmierkowski, "Direct power control of an AFE using predictive control," *IEEE Trans. Power Electron.*, vol. 23, no. 5, pp. 2516–2523, Sep. 2008.

[23] D. E. Quevedo, R. P. Aguilera, M. A. Pérez, P. Cortés, and R. Lizana, "Model predictive control of an AFE rectifier with dynamic references," *IEEE Trans. Power Electron.*, vol. 27, no. 7, pp. 3128–3136, Jul. 2012.

[24] J. Rodríguez, R. M. Kennel, J. R. Espinoza, M. Trincado, C. A. Silva, and C. A. Rojas, "High-performance control strategies for electrical drives: An experimental assessment," *IEEE Trans. Ind. Electron.*, vol. 59, no. 2, pp. 812–820, Feb. 2012.

[25] V. Yaramasu and B. Wu, "Predictive control of a three-level boost converter and an NPC inverter for high-power PMSG-based medium voltage wind energy conversion systems," *IEEE Trans. Power Electron.*, vol. 29, no. 10, pp. 5308–5322, Oct. 2014.

[26] T. Geyer and D. E. Quevedo, "Multistep finite control set model predictive control for power electronics," *IEEE Trans. Power Electron.*, vol. 29, no. 12, pp. 6836–6846, Dec. 2014.

[27] M. Narimani, B. Wu, V. Yaramasu, Z. Cheng, and N. R. Zargari, "Finite control-set model predictive control (FCS-MPC) of nested neutral point-clamped (NNPC) converter," *IEEE Trans. Power Electron.*, vol. 30, no. 12, pp. 7262–7269, Dec. 2015.

[28] K. Antoniewicz, M. Jasinski, M. P. Kazmierkowski, and M. Malinowski, "Model predictive control for three-level four-leg flying capacitor converter operating as shunt active power filter," *IEEE Trans. Ind. Electron.*, vol. 63, no. 8, pp. 5255–5262, Aug. 2016.

[29] A. Dekka, B. Wu, V. Yaramasu, and N. R. Zargari, "Model predictive control with common-mode voltage injection for modular multilevel converter," *IEEE Trans. Power Electron.*, vol. 32, no. 3, pp. 1767–1778, Mar. 2017.

[30] Z. Zhang, C. M. Hackl, and R. Kennel, "Computationally efficient DMPC for three-level NPC back-to-back converters in wind turbine systems with PMSG," *IEEE Trans. Power Electron.*, vol. 32, no. 10, pp. 8018–8034, Oct. 2017.

[31] M. Siami, D. A. Khaburi, and J. Rodríguez, "Simplified finite control set-model predictive control for matrix converter-fed PMSM drives," *IEEE Trans. Power Electron.*, vol. 33, no. 3, pp. 2438–2446, Mar. 2018.

[32] C. Zheng, T. Dragičević, and F. Blaabjerg, "Current-sensorless finite-set model predictive control for LC-filtered voltage source inverters," *IEEE Trans. Power Electron.*, vol. 35, no. 1, pp. 1086–1095, Jan. 2020.

[33] P. Karamanakos and T. Geyer, "Guidelines for the design of finite control set model predictive controllers," *IEEE Trans. Power Electron.*, vol. 35, no. 7, pp. 7434–7450, Jul. 2020.

[34] J. Holtz and S. Stadtfeld, "Field-oriented control by forced motor currents in a voltage fed inverter drive," in *IFAC Symp.*, Lausanne, Switzerland, Sep. 1983, pp. 103–110.

[35] ——, "An economic very high power PWM inverter for induction motor drives," in *Proc. Eur. Power Electron. Conf.*, Brussels, Belgium, Oct. 1985, pp. 3.75–3.89.

[36] J. W. Kolar, H. Ertl, and F. C. Zach, "Analysis of on- and off-line optimized predictive current controllers for PWM converter systems," *IEEE Trans. Power Electron.*, vol. 6, no. 3, pp. 451–462, Jul. 1991.

[37] M. Pacas and J. Weber, "Predictive direct torque control for the PM synchronous machine," *IEEE Trans. Ind. Electron.*, vol. 52, no. 5, pp. 1350–1356, Oct. 2005.

[38] T. Geyer, "Low complexity model predictive control in power electronics and power systems," Ph.D. dissertation, Autom. Control Lab. ETH Zurich, Zurich, Switzerland, 2005.

[39] T. Geyer, G. Papafotiou, and M. Morari, "Model predictive direct torque control—Part I: Concept, algorithm and analysis," *IEEE Trans. Ind. Electron.*, vol. 56, no. 6, pp. 1894–1905, Jun. 2009.

[40] G. Papafotiou, J. Kley, K. G. Papadopoulos, P. Bohren, and M. Morari, "Model predictive direct torque control—Part II: Implementation and experimental evaluation," *IEEE Trans. Ind. Electron.*, vol. 56, no. 6, pp. 1906–1915, Jun. 2009.

[41] T. Geyer, "Generalized model predictive direct torque control: Long prediction horizons and minimization of switching losses," in *Proc. IEEE Conf. Decis. Control*, Shanghai, China, Dec. 2009, pp. 6799–6804.

[42] ——, "Computationally efficient model predictive direct torque control," *IEEE Trans. Power Electron.*, vol. 26, no. 10, pp. 2804–2816, Oct. 2011.

[43] T. Geyer and S. Mastellone, "Model predictive direct torque control of a five-level ANPC converter drive system," *IEEE Trans. Ind. Appl.*, vol. 48, no. 5, pp. 1565–1575, Sep./Oct. 2012.

[44] B. S. Riar, T. Geyer, and U. K. Madawala, "Model predictive direct current control of modular multilevel converters: Modeling, analysis, and experimental evaluation," *IEEE Trans. Power Electron.*, vol. 30, no. 1, pp. 431–439, Jan. 2015.

[45] J. Scoltock, T. Geyer, and U. K. Madawala, "Model predictive direct power control for grid-connected NPC converters," *IEEE Trans. Ind. Electron.*, vol. 62, no. 9, pp. 5319–5328, Sep. 2015.

[46] ——, "A model predictive direct current control strategy with predictive references for MV grid-connected converters with LCL-filters," *IEEE Trans. Power Electron.*, vol. 30, no. 10, pp. 5926–5937, Oct. 2015.

[47] J. Beerten, J. Verveckken, and J. Driesen, "Predictive direct torque control for flux and torque ripple reduction," *IEEE Trans. Ind. Electron.*, vol. 57, no. 1, pp. 404–412, Jan. 2010.

[48] T. Geyer, "Model predictive direct current control: Formulation of the stator current bounds and the concept of the switching horizon," *IEEE Ind. Appl. Mag.*, vol. 18, no. 2, pp. 47–59, Mar./Apr. 2012.

[49] P. Landsmann and R. Kennel, "Saliency-based sensorless predictive torque control with reduced torque ripple," *IEEE Trans. Power Electron.*, vol. 27, no. 10, pp. 4311–4320, Oct. 2012.

[50] P. Karamanakos, P. Stolze, R. M. Kennel, S. Manias, and H. du T. Mouton, "Variable switching point predictive torque control of induction machines," *IEEE J. Emerg. Sel. Topics Power Electron.*, vol. 2, no. 2, pp. 285–295, Jun. 2014.

[51] L. Tarisciotti, P. Zanchetta, A. Watson, S. Bifaretti, and J. C. Clare, "Modulated model predictive control for a seven-level cascaded H-bridge back-to-back converter," *IEEE Trans. Ind. Electron.*, vol. 61, no. 10, pp. 5375–5383, Oct. 2014.

[52] Y. Zhang, W. Xie, Z. Li, and Y. Zhang, "Low-complexity model predictive power control: Double-vector-based approach," *IEEE Trans. Ind. Electron.*, vol. 61, no. 11, pp. 5871–5880, Nov. 2014.

[53] S. Vazquez, A. Marquez, R. Aguilera, D. Quevedo, J. I. Leon, and L. G. Franquelo, "Predictive optimal switching sequence direct power control for grid-connected power converters," *IEEE Trans. Ind. Electron.*, vol. 62, no. 4, pp. 2010–2020, Apr. 2015.

[54] Y. Zhang, Y. Peng, and C. Qu, "Model predictive control and direct power control for PWM rectifiers with active power ripple minimization," *IEEE Trans. Ind. Appl.*, vol. 52, no. 6, pp. 4909–4918, Nov./Dec. 2016.

[55] Y. Zhang, D. Xu, J. Liu, S. Gao, and W. Xu, "Performance improvement of model-predictive current control of permanent magnet synchronous motor drives," *IEEE Trans. Ind. Appl.*, vol. 53, no. 4, pp. 3683–3695, Jul./Aug. 2017.

[56] F. Donoso, A. Mora, R. Cárdenas, A. Angulo, D. Sáez, and M. Rivera, "Finite-set model predictive control strategies for a 3L-NPC inverter operating with fixed switching frequency," *IEEE Trans. Ind. Electron.*, vol. 65, no. 5, pp. 3954–3965, May 2018.

[57] Y. Zhang, Y. Bai, and H. Yang, "A universal multiple-vector-based model predictive control of induction motor drives," *IEEE Trans. Power Electron.*, vol. 33, no. 8, pp. 6957–6969, Aug. 2018.

[58] P. Karamanakos, A. Ayad, and R. Kennel, "A variable switching point predictive current control strategy for quasi-Z-source inverters," *IEEE Trans. Ind. Appl.*, vol. 54, no. 2, pp. 1469–1480, Mar./Apr. 2018.

[59] A. Mora, R. Cárdenas-Dobson, R. P. Aguilera, A. Angulo, F. Donoso, and J. Rodríguez, "Computationally efficient cascaded optimal switching sequence MPC for grid-connected three-level NPC converters," *IEEE Trans. Power Electron.*, vol. 34, no. 12, pp. 12 464–12 475, Dec. 2019.

[60] S. Vazquez, P. Acuña, R. P. Aguilera, J. Pou, J. I. Leon, and L. G. Franquelo, "Dc-link voltage balancing strategy based on optimal switching sequences model predictive control for single-phase H-NPC converters," *IEEE Trans. Ind. Electron.*, vol. 67, no. 9, pp. 7410–7420, Sep. 2020.

[61] L. Tarisciotti, P. Zanchetta, A. Watson, J. C. Clare, M. Degano, and S. Bifaretti, "Modulated model predictive control for a three-phase active rectifier," *IEEE Trans. Ind. Appl.*, vol. 51, no. 2, pp. 1610–1620, Mar./Apr. 2015.

[62] M. Tomlinson, H. du T. Mouton, R. Kennel, and P. Stolze, "A fixed switching frequency scheme for finite-control-set model predictive control—Concept and algorithm," *IEEE Trans. Ind. Electron.*, vol. 63, no. 12, pp. 7662–7670, Dec. 2016.

[63] S. Vazquez, R. P. Aguilera, P. Acuna, J. Pou, J. I. Leon, L. G. Franquelo, and V. G. Agelidis, "Model predictive control for single-phase NPC converters based on optimal switching sequences," *IEEE Trans. Ind. Electron.*, vol. 63, no. 12, pp. 7533–7541, Dec. 2016.

[64] L. Tarisciotti, A. Formentini, A. Gaeta, M. Degano, P. Zanchetta, R. Rabbeni, and M. Pucci, "Model predictive control for shunt active filters with fixed switching frequency," *IEEE Trans. Ind. Appl.*, vol. 53, no. 1, pp. 296–304, Jan./Feb. 2017.

[65] M. Vijayagopal, P. Zanchetta, L. Empringham, L. de Lillo, L. Tarisciotti, and P. Wheeler, "Control of a direct matrix converter with modulated model-predictive control," *IEEE Trans. Ind. Appl.*, vol. 53, no. 3, pp. 2342–2349, May/Jun. 2017.

[66] L. Tarisciotti, J. Lei, A. Formentini, A. Trentin, P. Zanchetta, P. Wheeler, and M. Rivera, "Modulated predictive control for indirect matrix converter," *IEEE Trans. Ind. Appl.*, vol. 53, no. 5, pp. 4644–4654, Sep./Oct. 2017.

[67] P. Karamanakos, R. Mattila, and T. Geyer, "Fixed switching frequency direct model predictive control based on output current gradients," in *Proc. IEEE Ind. Electron. Conf.*, Washington, D.C., USA, Oct. 2018, pp. 2329–2334.

[68] C. Zheng, T. Dragičević, B. Majmunović, and F. Blaabjerg, "Constrained modulated-model predictive control of an LC-filtered voltage source converter," *IEEE Trans. Power Electron.*, vol. 35, no. 2, pp. 1967–1977, Feb. 2020.

[69] D. G. Holmes and T. A. Lipo, *Pulse width modulation for power converters: Principles and practice*. Piscataway, NJ, USA: IEEE Press, 2003.

[70] H. S. Patel and R. G. Hoft, "Generalized techniques of harmonic elimination and voltage control in thyristor inverters: Part I—Harmonic elimination," *IEEE Trans. Ind. Appl.*, vol. IA-9, no. 3, pp. 310–317, May 1973.

[71] ——, "Generalized techniques of harmonic elimination and voltage control in thyristor inverters: Part II—Voltage control techniques," *IEEE Trans. Ind. Appl.*, vol. IA-10, no. 5, pp. 666–673, Sep. 1974.

[72] G. S. Buja and G. B. Indri, "Optimal pulsewidth modulation for feeding ac motors," *IEEE Trans. Ind. Appl.*, vol. IA-13, no. 1, pp. 38–44, Jan. 1977.

[73] G. S. Buja, "Optimum output waveforms in PWM inverters," *IEEE Trans. Ind. Appl.*, vol. IA-16, no. 6, pp. 830–836, Nov./Dec. 1980.

[74] J. Holtz and B. Beyer, "The trajectory tracking approach—A new method for minimum distortion PWM in dynamic high-power drives," *IEEE Trans. Ind. Appl.*, vol. 30, no. 4, pp. 1048–1057, Jul./Aug. 1994.

[75] ——, "Fast current trajectory tracking control based on synchronous optimal pulsewidth modulation," *IEEE Trans. Ind. Appl.*, vol. 31, no. 5, pp. 1110–1120, Sep./Oct. 1995.

[76] J. Holtz and N. Oikonomou, "Synchronous optimal pulsewidth modulation and stator flux trajectory control for medium-voltage drives," *IEEE Trans. Ind. Appl.*, vol. 43, no. 2, pp. 600–608, Mar./Apr. 2007.

[77] N. Oikonomou and J. Holtz, "Closed-loop control of medium-voltage drives operated with synchronous optimal pulsewidth modulation," *IEEE Trans. Ind. Appl.*, vol. 44, no. 1, pp. 115–123, Jan./Feb. 2008.

[78] J. Holtz and N. Oikonomou, "Estimation of the fundamental current in low-switching-frequency high dynamic medium voltage drives," *IEEE Trans. Ind. Appl.*, vol. 44, no. 5, pp. 1597–1605, Sep./Oct. 2008.

[79] T. Geyer, N. Oikonomou, G. Papafotiou, and F. D. Kieferndorf, "Model predictive pulse pattern control," *IEEE Trans. Ind. Appl.*, vol. 48, no. 2, pp. 663–676, Mar./Apr. 2012.

[80] N. Oikonomou, C. Gutscher, P. Karamanakos, F. D. Kieferndorf, and T. Geyer, "Model predictive pulse pattern control for the five-level active neutral-point-clamped inverter," *IEEE Trans. Ind. Appl.*, vol. 49, no. 6, pp. 2583–2592, Nov./Dec. 2013.

[81] M. Vasiladiotis, A. Christe, and T. Geyer, "Model predictive pulse pattern control for modular multilevel converters," *IEEE Trans. Ind. Electron.*, vol. 66, no. 3, pp. 2423–2431, Mar. 2019.

[82] R. P. Aguilera, P. Acuña, P. Lezana, G. Konstantinou, B. Wu, S. Bernet, and V. G. Agelidis, "Selective harmonic elimination model predictive control for multilevel power converters," *IEEE Trans. Power Electron.*, vol. 32, no. 3, pp. 2416–2426, Mar. 2017.

[83] H. Gao, B. Wu, D. Xu, R. P. Aguilera, and P. Acuña, "Model predictive switching pattern control for current-source converters with space-vector-based selective harmonic elimination," *IEEE Trans. Power Electron.*, vol. 32, no. 8, pp. 6558–6569, Aug. 2017.

[84] M. Wu, H. Tian, Y. Li, G. Konstantinou, and K. Yang, "A composite selective harmonic elimination model predictive control for seven-level hybrid-clamped inverters with optimal switching patterns," *IEEE Trans. Power Electron.*, pp. 1–11, 2020, in press, DOI: 10.1109/TPEL.2020.3002968.

[85] J. Holtz, "Pulsewidth modulation—A survey," *IEEE Trans. Ind. Electron.*, vol. 39, no. 5, pp. 410–420, Oct. 1992.

[86] ——, "Pulsewidth modulation for electronic power conversion," *Proc. IEEE*, vol. 82, no. 8, pp. 1194–1124, Aug. 1994.

[87] F. Borrelli, M. Baotić, A. Bemporad, and M. Morari, "Dynamic programming for constrained optimal control of discrete-time linear hybrid systems," *Automatica*, vol. 41, no. 10, pp. 1709–1721, Oct. 2005.

[88] F. Borrelli, A. Bemporad, and M. Morari, *Predictive control for linear and hybrid systems*. Cambridge, UK: Cambridge Univ. Press, 2011.

[89] L. A. Wolsey, *Integer programming*. New York, NY, USA: Wiley, 1998.

[90] T. Geyer, G. Papafotiou, R. Frasca, and M. Morari, "Constrained optimal control of the step-down dc-dc converter," *IEEE Trans. Power Electron.*, vol. 23, no. 5, pp. 2454–2464, Sep. 2008.

[91] S. Mariéthoz and M. Morari, "Explicit model-predictive control of a PWM inverter with an LCL filter," *IEEE Trans. Ind. Electron.*, vol. 56, no. 2, pp. 389–399, Feb. 2009.

[92] S. Bolognani, S. Bolognani, L. Peretti, and M. Zigliotto, "Design and implementation of model predictive control for electrical motor drives," *IEEE Trans. Ind. Electron.*, vol. 56, no. 6, pp. 1925–1936, Jun. 2009.

[93] A. G. Beccuti, S. Mariéthoz, S. Cliquennois, S. Wang, and M. Morari, "Explicit model predictive control of dc-dc switched-mode power supplies with extended Kalman filtering," *IEEE Trans. Ind. Electron.*, vol. 56, no. 6, pp. 1864–1874, Jun. 2009.

[94] S. Mariéthoz, A. Domahidi, and M. Morari, "High-bandwidth explicit model predictive control of electrical drives," *IEEE Trans. Ind. Appl.*, vol. 48, no. 6, pp. 1980–1992, Nov./Dec. 2012.

[95] G. Beccuti, G. Papafotiou, and L. Harnefors, "Multivariable optimal control of HVDC transmission links with network parameter estimation for weak grids," *IEEE Trans. Control Syst. Technol.*, vol. 22, no. 2, pp. 676–689, Mar. 2014.

[96] K. Belda and D. Vošmik, "Explicit generalized predictive control of speed and position of PMSM drives," *IEEE Trans. Ind. Electron.*, vol. 63, no. 6, pp. 3889–3896, Jun. 2016.

[97] M. Jofré, A. M. Llor, and C. A. Silva, "Sensorless low switching frequency explicit model predictive control of induction machines fed by neutral point clamped inverter," *IEEE Trans. Ind. Electron.*, vol. 66, no. 12, pp. 9122–9128, Dec. 2019.

[98] J. Chen, Y. Chen, L. Tong, L. Peng, and Y. Kang, "A backpropagation neutral network based explicit model predictive control for dc-dc converters with high switching frequency," *IEEE J. Emerg. Sel. Topics Power Electron.*, vol. 8, no. 3, pp. 2124–2142, Sep. 2020.

[99] G. Darivianakis, T. Geyer, and W. van der Merwe, "Model predictive current control of modular multilevel converters," in *Proc. IEEE Energy Convers. Congr. Expo.*, Pittsburgh, PA, USA, Sep. 2014, pp. 5016–5023.

[100] S. Hanke, O. Wallscheid, and J. Böcker, "Continuous-control-set model predictive control with integrated modulator in permanent magnet synchronous motor applications," in *Proc. IEEE Int. Elect. Mach. Drives Conf.*, San Diego, CA, USA, May 2019, pp. 2210–2216.

[101] F. Toso, P. G. Carlet, A. Favato, and S. Bolognani, "On-line continuous control set MPC for PMSM drives current loops at high sampling rate using qpOASES," in *Proc. IEEE Energy Convers. Congr. Expo.*, Baltimore, MD, USA, Sep./Oct. 2019, pp. 6615–6620.

[102] G. Cimini, D. Bernardini, S. Levijoki, and A. Bemporad, "Embedded model predictive control with certified real-time optimization for synchronous motors," *IEEE Trans. Control Syst. Technol.*, pp. 1–8, 2020, in press, DOI: 10.1109/TCST.2020.2977295.

[103] O. Wallscheid and E. F. B. Ngoumtsa, "Investigation of disturbance observers for model predictive current control in electric drives," *IEEE Trans. Power Electron.*, pp. 1–9, 2020, in press, DOI: 10.1109/TPEL.2020.2992784.

[104] M. Rossi, P. Karamanakos, and F. Castelli-Dezza, "Indirect model predictive control for a grid-tied three-level neutral point clamped converter with an LCL filter," in *Proc. IEEE Energy Convers. Congr. Expo.*, Detroit, MI, USA, Oct. 2020, pp. 1–8.

[105] C. M. Hackl, "MPC with analytical solution and integral error feedback for LTI MIMO systems and its application to current control of grid-connected power converters with LCL-filter," in *Proc. IEEE Int. Symp. Pred. Control of Elect. Drives and Power Electron.*, Valparaíso, Chile, Oct. 2015, pp. 61–66.

[106] C. Dirscherl and C. M. Hackl, "Model predictive current control with analytical solution and integral error feedback of doubly-fed induction generators with LC filter," in *Proc. IEEE Int. Symp. Pred. Control of Elect. Drives and Power Electron.*, Pilsen, Czech Republic, Sep. 2017, pp. 25–30.

[107] J. Ma, W. Song, S. Wang, and X. Feng, "Model predictive direct power control for single phase three-level rectifier at low switching frequency," *IEEE Trans. Power Electron.*, vol. 33, no. 2, pp. 1050–1062, Feb. 2018.

[108] H. T. Nguyen, E.-K. Kim, I.-P. Kim, H. H. Choi, and J.-W. Jung, "Model predictive control with modulated optimal vector for a three-phase inverter with an LC filter," *IEEE Trans. Power Electron.*, vol. 33, no. 3, pp. 2690–2703, Mar. 2018.

[109] C. Bruni, G. Di Pillo, and G. Koch, "Bilinear systems: An appealing class of "nearly linear" systems in theory and applications," *IEEE Trans. Autom. Control*, vol. AC-19, no. 4, pp. 334–348, Aug. 1974.

[110] P. Karamanakos, T. Geyer, and S. Manias, "Direct voltage control of dc-dc boost converters using enumeration-based model predictive control," *IEEE Trans. Power Electron.*, vol. 29, no. 2, pp. 968–978, Feb. 2014.

[111] S.-K. Kim, C. R. Park, J.-S. Kim, and Y. I. Lee, "A stabilizing model predictive controller for voltage regulation of a dc/dc boost converter," *IEEE Trans. Control Syst. Technol.*, vol. 22, no. 5, pp. 2016–2023, Sep. 2014.

[112] A. M. Lopez, D. E. Quevedo, R. P. Aguilera, T. Geyer, and N. Oikonomou, "Limitations and accuracy of a continuous reduced-order model for modular multilevel converters," *IEEE Trans. Power Electron.*, vol. 33, no. 7, pp. 6292–6303, Jul. 2018.

[113] Y. Zhang, H. Yang, and B. Xia, "Model-predictive control of induction motor drives: Torque control versus flux control," *IEEE Trans. Ind. Appl.*, vol. 52, no. 5, pp. 4050–4060, Sep./Oct. 2016.

[114] H. Miranda, P. Cortés, J. I. Yuz, and J. Rodríguez, "Predictive torque control of induction machines based on state-space models," *IEEE Trans. Ind. Electron.*, vol. 56, no. 6, pp. 1916–1924, Jun. 2009.

[115] P. Karamanakos and T. Geyer, "Model predictive torque and flux control minimizing current distortions," *IEEE Trans. Power Electron.*, vol. 34, no. 3, pp. 2007–2012, Mar. 2019.

[116] P. Karamanakos, K. Pavlou, and S. Manias, "An enumeration-based model predictive control strategy for the cascaded H-bridge multilevel rectifier," *IEEE Trans. Ind. Electron.*, vol. 61, no. 7, pp. 3480–3489, Jul. 2014.

[117] Y. Zhang, X. Wu, X. Yuan, Y. Wang, and P. Dai, "Fast model predictive control for multilevel cascaded H-bridge STATCOM with polynomial computation time," *IEEE Trans. Ind. Electron.*, vol. 63, no. 8, pp. 5231–5243, Aug. 2016.

[118] D.-K. Choi and K.-B. Lee, "Dynamic performance improvement of ac/dc converter using model predictive direct power control with finite control set," *IEEE Trans. Ind. Electron.*, vol. 62, no. 2, pp. 757–767, Feb. 2015.

[119] P. Correa, J. Rodríguez, I. Lizama, and D. Andler, "A predictive control scheme for current-source rectifiers," *IEEE Trans. Ind. Electron.*, vol. 56, no. 5, pp. 1813–1815, May 2009.

[120] P. Falkowski and A. Sikorski, "Finite control set model predictive control for grid-connected ac-dc converters with LCL filter," *IEEE Trans. Ind. Electron.*, vol. 65, no. 4, pp. 2844–2852, Apr. 2018.

[121] P. Karamanakos, M. Nahalparvari, and T. Geyer, "Fixed switching frequency direct model predictive control with continuous and discontinuous modulation for grid-tied converters with LCL filters," *IEEE Trans. Control Syst. Technol.*, pp. 1–16, 2020, in press, DOI: 10.1109/TCST.2020.3008030.

[122] P. Cortés, G. Ortiz, J. I. Yuz, J. Rodríguez, S. Vazquez, and L. G. Franquelo, "Model predictive control of an inverter with output LC filter for UPS applications," *IEEE Trans. Ind. Electron.*, vol. 56, no. 6, pp. 1875–1883, Jun. 2009.

[123] J. Qin and M. Saeedifard, "Predictive control of a modular multilevel converter for a back-to-back HVDC system," *IEEE Trans. Power Del.*, vol. 27, no. 3, pp. 1538–1647, Jul. 2012.

[124] R. Vargas, U. Ammann, and J. Rodríguez, "Predictive approach to increase efficiency and reduce switching losses on matrix converters," *IEEE Trans. Power Electron.*, vol. 24, no. 4, pp. 894–902, Apr. 2009.

[125] M. Rivera, C. Rojas, J. Rodríguez, P. Wheeler, B. Wu, and J. Espinoza, "Predictive current control with input filter resonance mitigation for a direct matrix converter," *IEEE Trans. Power Electron.*, vol. 26, no. 10, pp. 2794–2803, Oct. 2011.

[126] M. Mosa, R. S. Balog, and H. Abu-Rub, "High performance predictive control of quasi impedance source inverter," *IEEE Trans. Power Electron.*, vol. 32, no. 4, pp. 3251–3262, Apr. 2017.

[127] A. Ayad, P. Karamanakos, and R. Kennel, "Direct model predictive current control strategy of quasi-Z-source inverters," *IEEE Trans. Power Electron.*, vol. 32, no. 7, pp. 5786–5801, Jul. 2017.

[128] H. Gao, B. Wu, D. Xu, and N. R. Zargari, "A model predictive power factor control scheme with active damping function for current source rectifiers," *IEEE Trans. Power Electron.*, vol. 33, no. 3, pp. 2655–2667, Mar. 2018.

[129] B. Stellato, T. Geyer, and P. J. Goulart, "High-speed finite control set model predictive control for power electronics," *IEEE Trans. Power Electron.*, vol. 32, no. 5, pp. 4007–4020, May 2017.

[130] M. Siami, D. A. Khaburi, M. Rivera, and J. Rodríguez, "A computationally efficient lookup table based FCS-MPC for PMSM drives fed by matrix converters," *IEEE Trans. Ind. Electron.*, vol. 64, no. 10, pp. 7645–7654, Oct. 2017.

[131] R. S. Palais and R. A. Palais, *Differential equations, mechanics, and computation*. Providence, RI, USA: Amer. Mathem. Soc., 2009.

[132] M. S. Asif and J. Romberg, "Fast and accurate algorithms for re-weighted ℓ_1-norm minimization," *IEEE Trans. Signal Proc.*, vol. 61, no. 23, pp. 5905–5916, Dec. 2013.

[133] M. A. Perez, J. Rodríguez, E. J. Fuentes, and F. Kammerer, "Predictive control of ac-ac modular multilevel converters," *IEEE Trans. Ind. Electron.*, vol. 59, no. 7, pp. 2832–2839, Jul. 2012.

[134] T. Geyer, P. Karamanakos, and R. Kennel, "On the benefit of long-horizon direct model predictive control for drives with LC filters," in *Proc. IEEE Energy Convers. Congr. Expo.*, Pittsburgh, PA, USA, Sep. 2014, pp. 3520–3527.

[135] C. A. Floudas, *Nonlinear and mixed-integer optimization: Fundamentals and applications*. Oxford, UK: Oxford Univ. Press, 1995.

[136] S. Boyd and L. Vandenberghe, *Convex optimization*. Cambridge, UK: Cambridge Univ. Press, 2004.

[137] P. Karamanakos, T. Geyer, N. Oikonomou, F. D. Kieferndorf, and S. Manias, "Direct model predictive control: A review of strategies that achieve long prediction intervals for power electronics," *IEEE Ind. Electron. Mag.*, vol. 8, no. 1, pp. 32–43, Mar. 2014.

[138] P. Karamanakos, T. Geyer, and R. Kennel, "A computationally efficient model predictive control strategy for linear systems with integer inputs," *IEEE Trans. Control Syst. Technol.*, vol. 24, no. 4, pp. 1463–1471, Jul. 2016.

[139] M. Abdelrahem, C. M. Hackl, and R. Kennel, "Finite position set-phase locked loop for sensorless control of direct-driven permanent-magnet synchronous generators," *IEEE Trans. Power Electron.*, vol. 33, no. 4, pp. 3097–3105, Apr. 2018.

[140] O. Sandre-Hernandez, J. Rangel-Magdaleno, and R. Morales-Caporal, "A comparison on finite-set model predictive torque control schemes for PMSMs," *IEEE Trans. Power Electron.*, vol. 33, no. 10, pp. 8838–8847, Oct. 2018.

[141] P. Karamanakos, T. Geyer, and R. Kennel, "On the choice of norm in finite control set model predictive control," *IEEE Trans. Power Electron.*, vol. 33, no. 8, pp. 7105–7117, Aug. 2018.

[142] T. Geyer and D. E. Quevedo, "Performance of multistep finite control set model predictive control for power electronics," *IEEE Trans. Power Electron.*, vol. 30, no. 3, pp. 1633–1644, Mar. 2015.

[143] T. Dragičević and M. Novak, "Weighting factor design in model predictive control of power electronic converters: An artificial neural network approach," *IEEE Trans. Ind. Electron.*, vol. 66, no. 11, pp. 8870–8880, Nov. 2019.

[144] A. Andersson and T. Thiringer, "Assessment of an improved finite control set model predictive current controller for automotive propulsion applications," *IEEE Trans. Ind. Electron.*, vol. 67, no. 1, pp. 91–100, Jan. 2020.

[145] Z. Zhang, F. Wang, T. Sun, J. Rodríguez, and R. Kennel, "FPGA-based experimental investigation of a quasi-centralized model predictive control for back-to-back converters," *IEEE Trans. Power Electron.*, vol. 31, no. 1, pp. 662–674, Jan. 2016.

[146] R. Baidya, R. P. Aguilera, P. Acuña, S. Vasquez, and H. du T. Mouton, "Multistep model predictive control for cascaded H-bridge inverters—Formulation and analysis," *IEEE Trans. Power Electron.*, vol. 33, no. 1, pp. 876–886, Jan. 2018.

[147] P. Acuña, C. Rojas, R. Baidya, R. P. Aguilera, and J. Fletcher, "On the impact of transients on multistep model predictive control for medium-voltage drives," *IEEE Trans. Power Electron.*, vol. 34, no. 9, pp. 8342–8355, Sep. 2019.

[148] S. Almér, S. Mariéthoz, and M. Morari, "Sampled data model predictive control of a voltage source inverter for reduced harmonic distortion," *IEEE Trans. Control Syst. Technol.*, vol. 21, no. 5, pp. 1907–1915, Sep. 2013.

[149] P. Cortés, S. Kouro, B. L. Rocca, R. Vargas, J. Rodríguez, J. I. León, S. Vazquez, and L. G. Franquelo, "Guidelines for weighting factors design in model predictive control of power converters and drives," in *Proc. IEEE Int. Conf. Ind. Technol.*, Gippsland, Australia, Feb. 2009, pp. 1–7.

[150] P. Zanchetta, "Heuristic multi-objective optimization for cost function weights selection in finite states model predictive control," in *Proc. Workshop on Pred. Control of Elect. Drives and Power Electron.*, Munich, Germany, Oct. 2011, pp. 70–75.

[151] S. A. Davari, D. A. Khaburi, and R. Kennel, "An improved FCS-MPC algorithm for an induction motor with an imposed optimized weighting factor," *IEEE Trans. Power Electron.*, vol. 27, no. 3, pp. 1540–1551, Mar. 2012.

[152] T. Geyer, "Algebraic tuning guidelines for model predictive torque and flux control," *IEEE Trans. Ind. Appl.*, vol. 54, no. 5, pp. 4464–4475, Sep./Oct. 2018.

[153] O. Machado, P. Martín, F. J. Rodríguez, and E. J. Bueno, "A neural network-based dynamic cost function for the implementation of a predictive current controller," *IEEE Trans. Ind. Informat.*, vol. 13, no. 6, pp. 2946–2955, Dec. 2017.

[154] M. B. Shadmand, S. Jain, and R. S. Balog, "Autotuning technique for the cost function weight factors in model predictive control for power electronic interfaces," *IEEE J. Emerg. Sel. Topics Power Electron.*, vol. 7, no. 2, pp. 1408–1420, Jun. 2019.

[155] P. R. U. Guazzelli, W. C. de Andrade Pereira, C. M. R. de Oliveira, A. G. de Castro, and M. L. de Aguiar, "Weighting factors optimization of predictive torque control of induction motor by multiobjective genetic algorithm," *IEEE Trans. Power Electron.*, vol. 34, no. 7, pp. 6628–6638, Jul. 2019.

[156] H. A. Young, M. A. Perez, and J. Rodríguez, "Analysis of finite-control-set model predictive current control with model parameter mismatch in a three-phase inverter," *IEEE Trans. Ind. Electron.*, vol. 63, no. 5, pp. 3100–3107, May 2016.

[157] R. P. Aguilera, P. Lezana, and D. E. Quevedo, "Finite-control-set model predictive control with improved steady-state performance," *IEEE Trans. Ind. Informat.*, vol. 9, no. 2, pp. 658–667, May 2013.

[158] M. Siami, D. A. Khaburi, A. Abbaszadeh, and J. Rodríguez, "Robustness improvement of predictive current control using prediction error correction for permanent-magnet synchronous machines," *IEEE Trans. Ind. Electron.*, vol. 63, no. 6, pp. 3458–3466, Jun. 2016.

[159] S. A. Davari, D. A. Khaburi, F. Wang, and R. Kennel, "Using full order and reduced order observers for robust sensorless predictive torque control of induction motors," *IEEE Trans. Power Electron.*, vol. 27, no. 7, pp. 3424–3433, Jul. 2012.

[160] J. Wang, F. Wang, G. Wang, S. Li, and L. Yu, "Generalized proportional integral observer based robust finite control set predictive current control for induction motor systems with time-varying disturbances," *IEEE Trans. Ind. Informat.*, vol. 14, no. 9, pp. 4159–4168, Sep. 2018.

[161] F. Toso, D. Da Rú, P. Alotto, and S. Bolognani, "A moving horizon estimator for the speed and rotor position of a sensorless PMSM drive," *IEEE Trans. Power Electron.*, vol. 34, no. 1, pp. 580–587, Jan. 2019.

[162] M. Yang, X. Lang, J. Long, and D. Xu, "Flux immunity robust predictive current control with incremental model and extended state observer for PMSM drive," *IEEE Trans. Power Electron.*, vol. 32, no. 12, pp. 9267–9279, Dec. 2017.

[163] X. Zhang, L. Zhang, and Y. Zhang, "Model predictive current control for PMSM drives with parameter robustness improvement," *IEEE Trans. Power Electron.*, vol. 34, no. 2, pp. 1645–1657, Feb. 2019.

[164] M. Khalilzadeh, S. Vaez-Zadeh, and M. S. Eslahi, "Parameter-free predictive control of IPM motor drives with direct selection of optimum

inverter voltage vectors," *IEEE J. Emerg. Sel. Topics Power Electron.*, pp. 1–8, 2020, in press, DOI: 10.1109/JESTPE.2019.2949222.
[165] C.-K. Lin, J.-t. Yu, Y.-S. Lai, and H.-C. Yu, "Improved model-free predictive current control for synchronous reluctance motor drives," *IEEE Trans. Ind. Electron.*, vol. 63, no. 6, pp. 3942–3953, Jun. 2016.
[166] D. Da Rú, M. Polato, and S. Bolognani, "Model-free predictive current control for a SynRM drive based on an effective update of measured current responses," in *Proc. IEEE Int. Symp. Pred. Control of Elect. Drives and Power Electron.*, Pilsen, Czech Republic, Sep. 2017, pp. 119–124.
[167] S. Hanke, S. Peitz, O. Wallscheid, J. Böcker, and M. Dellnitz, "Finite-control-set model predictive control for a permanent magnet synchronous motor application with online least squares system identification," in *Proc. IEEE Int. Symp. Pred. Control of Elect. Drives and Power Electron.*, Quanzhou, China, May/Jun. 2019, pp. 1–6.
[168] F. Tinazzi, P. G. Carlet, S. Bolognani, and M. Zigliotto, "Motor parameter-free predictive current control of synchronous motors by recursive least square self-commissioning model," *IEEE Trans. Ind. Electron.*, vol. 67, no. 11, pp. 9093–9100, Nov. 2020.
[169] H. K. Khalil, *Nonlinear Systems*, 3rd ed. Upper Saddle River, NJ, USA: Prentice-Hall, 2001.
[170] P. O. M. Scokaert, D. Q. Mayne, and J. B. Rawlings, "Suboptimal model predictive control (feasibility implies stability)," *IEEE Trans. Autom. Control*, vol. 44, no. 3, pp. 648–654, Mar. 1999.
[171] D. Q. Mayne, J. B. Rawlings, C. V. Rao, and P. O. M. Scokaert, "Constrained model predictive control: Stability and optimality," *Automatica*, vol. 36, no. 6, pp. 789–814, Jun. 2000.
[172] T. Geyer, G. Papafotiou, and M. Morari, "Hybrid model predictive control of the step-down dc-dc converter," *IEEE Trans. Control Syst. Technol.*, vol. 16, no. 6, pp. 1112–1124, Nov. 2008.
[173] O. Andres-Martinez, A. Flores-Tlacuahuac, O. F. Ruiz-Martinez, and J. C. Mayo-Maldonado, "Nonlinear model predictive stabilization of dc-dc boost converters with constant power loads," *IEEE J. Emerg. Sel. Topics Power Electron.*, pp. 1–8, 2020, in press, DOI: 10.1109/JESTPE.2020.2964674.
[174] R. P. Aguilera and D. E. Quevedo, "Stability analysis of quadratic MPC with a discrete input alphabet," *IEEE Trans. Autom. Control*, vol. 58, no. 12, pp. 3190–3196, Dec. 2013.
[175] ——, "Predictive control of power converters: Designs with guaranteed performance," *IEEE Trans. Ind. Informat.*, vol. 11, no. 1, pp. 53–63, Feb. 2015.
[176] M. P. Akter, S. Mekhilef, N. M. L. Tan, and H. Akagi, "Modified model predictive control of a bidirectional ac-dc converter based on Lyapunov function for energy storage systems," *IEEE Trans. Ind. Electron.*, vol. 63, no. 2, pp. 704–715, Feb. 2016.
[177] K. S. Alam, M. P. Akter, D. Xiao, D. Zhang, and M. F. Rahman, "Asymptotically stable predictive control of grid-connected converter based on discrete space vector modulation," *IEEE Trans. Ind. Informat.*, vol. 15, no. 5, pp. 2775–2785, May 2019.
[178] H. T. Nguyen and J.-W. Jung, "Asymptotic stability constraints for direct horizon-one model predictive control of SPMSM drives," *IEEE Trans. Power Electron.*, vol. 33, no. 10, pp. 8213–8219, Oct. 2018.
[179] M. Novak, U. M. Nyman, T. Dragičević, and F. Blaabjerg, "Analytical design and performance validation of finite set MPC regulated power converters," *IEEE Trans. Ind. Electron.*, vol. 66, no. 3, pp. 2004–2014, Mar. 2019.
[180] T. Geyer, R. P. Aguilera, and D. E. Quevedo, "On the stability and robustness of model predictive direct current control," in *Proc. IEEE Int. Conf. Ind. Technol.*, Cape Town, South Africa, Feb. 2013, pp. 374–379.
[181] P. Karamanakos, T. Geyer, and R. P. Aguilera, "Long-horizon direct model predictive control: Modified sphere decoding for transient operation," *IEEE Trans. Ind. Appl.*, vol. 54, no. 6, pp. 6060–6070, Nov./Dec. 2018.
[182] M. Dorfling, H. Mouton, T. Geyer, and P. Karamanakos, "Long-horizon finite-control-set model predictive control with non-recursive sphere decoding on an FPGA," *IEEE Trans. Power Electron.*, vol. 35, no. 7, pp. 7520–7531, Jul. 2020.
[183] B. Stellato, V. V. Naik, A. Bemporad, P. Goulart, and S. Boyd, "Embedded mixed-integer quadratic optimization using the OSQP solver," in *Proc. of the Eur. Control Conf.*, Limassol, Cyprus, Jun. 2018, pp. 1536–1541.
[184] R. Takapoui, N. Moehle, S. Boyd, and A. Bemporad, "A simple effective heuristic for embedded mixed-integer quadratic programming," *Int. J. of Control*, vol. 93, no. 1, pp. 2–12, 2020.
[185] D. Kouzoupis, A. Zanelli, H. Peyrl, and H. J. Ferreau, "Towards proper assessment of QP algorithms for embedded model predictive control," in *Proc. of the Eur. Control Conf.*, Linz, Austria, Jul. 2015, pp. 2609–2616.
[186] I. McInerney, G. A. Constantinides, and E. C. Kerrigan, "A survey of the implementation of linear model predictive control on FPGAs," in *IFAC Conf. on Nonlin. Model Pred. Control*, Madison, WI, USA, Aug. 2018, pp. 381–387.
[187] H. J. Ferreau, C. Kirches, A. Potschka, H. G. Bock, and M. Diehl, "qpOASES: A parametric active-set algorithm for quadratic programming," *Math. Program. Comp.*, vol. 6, no. 4, pp. 327–363, Dec. 2014.
[188] B. Hauska, H. J. Ferreau, and M. Diehl, "An auto-generated real-time iteration algorithm for nonlinear MPC in the microsecond range," *Automatica*, vol. 47, no. 10, pp. 2279–2285, Oct. 2011.
[189] J. A. E. Andersson, J. Gillis, G. Horn, J. B. Rawlings, and M. Diehl, "CasADi: A software framework for nonlinear optimization and optimal control," *Math. Program. Comp.*, vol. 11, no. 1, pp. 1–36, Mar. 2019.
[190] T. J. Besselmann, S. Almér, and H. J. Ferreau, "Model predictive control of load-commutated inverter-fed synchronous machines," *IEEE Trans. Power Electron.*, vol. 31, no. 10, pp. 7384–7393, Oct. 2016.
[191] T. J. Besselmann, S. Van de moortel, S. Almér, P. Jörg, and H. J. Ferreau, "Model predictive control in the multi-megawatt range," *IEEE Trans. Ind. Electron.*, vol. 63, no. 7, pp. 4641–4648, Jul. 2016.
[192] A. Zanelli, J. Kullick, H. Eldeeb, G. Frison, C. Hackl, and M. Diehl, "Continuous control set nonlinear model predictive control of reluctance synchronous machines," 2019.
[193] S. Wendel, A. Dietz, and R. Kennel, "FPGA based finite-set model predictive current control for small PMSM drives with efficient resource streaming," in *Proc. IEEE Int. Symp. Pred. Control of Elect. Drives and Power Electron.*, Pilsen, Czech Republic, Sep. 2019, pp. 66–71.
[194] A. Galassini, G. Lo Calzo, A. Formentini, C. Gerada, P. Zanchetta, and A. Costabeber, "uCube: Control platform for power electronics," in *Proc. IEEE Workshop on Elect. Mach. Design, Control and Diagn.*, Nottingham, UK, Apr. 2017, pp. 216–221.
[195] R. Schwendemann, S. Decker, M. Hiller, and M. Braun, "A modular converter- and signal-processing-platform for academic research in the field of power electronics," in *Proc. IEEE Int. Conf. Power Electron. and ECCE Asia*, Niigata, Japan, May 2018, pp. 3074–3080.
[196] A. Montazeri and G. Griepentrog, "Explicit consideration of inverter losses in the cost function for finite control set model predictive control of induction machine, experimental results," in *Proc. IEEE Int. Symp. Ind. Electron.*, Vancouver, BC, Canada, Jun. 2019, pp. 521–526.
[197] E. Zafra, S. Vazquez, H. Guzman Miranda, J. A. Sanchez, A. Marquez, J. I. Leon, and L. G. Franquelo, "Efficient FPSoC prototyping of FCS-MPC for three-phase voltage source inverters," *Energies*, vol. 13, no. 5, pp. 1–16, Mar. 2020.
[198] S. Wendel, A. Geiger, E. Liegmann, D. Arancibia, E. Durán, T. Kreppel, F. Rojas, F. Popp-Nowak, M. Diaz, A. Dietz, R. Kennel, and B. Wagner, "UltraZohm—A powerful real-time computation platform for MPC and multi-level inverters," in *Proc. IEEE Int. Symp. Pred. Control of Elect. Drives and Power Electron.*, Quanzhou, China, May/Jun. 2019, pp. 1–6.
[199] H.-J. Yoo, T.-T. Nguyen, and H.-M. Kim, "MPC with constant switching frequency for inverter-based distributed generations in microgrid using gradient descent," *Energies*, vol. 12, no. 6, pp. 1–14, Mar. 2019.
[200] P. Stolze, P. Karamanakos, R. Kennel, S. Manias, and C. Endisch, "Effective variable switching point predictive current control for ac low-voltage drives," *Int. J. of Control*, vol. 88, no. 7, pp. 1366–1378, Jul. 2015.
[201] IEEE Std 519-2014 (Revision of IEEE Std 519-1992), "IEEE recommended practices and requirements for harmonic control in electrical power systems," pp. 1–29, Jun. 2014.
[202] G. A. Papafotiou, G. D. Demetriades, and V. G. Agelidis, "Technology readiness assessment of model predictive control in medium- and high-voltage power electronics," *IEEE Trans. Ind. Electron.*, vol. 63, no. 9, pp. 5807–5815, Sep. 2016.
[203] E. Liegmann, P. Karamanakos, T. Geyer, T. Mouton, and R. Kennel, "Long-horizon direct model predictive control with active balancing of the neutral point potential," in *Proc. IEEE Int. Symp. Pred. Control of Elect. Drives and Power Electron.*, Pilsen, Czech Republic, Sep. 2017, pp. 89–94.
[204] D. Limon, A. Ferramosca, I. Alvarado, and T. Alamo, "Nonlinear MPC for tracking piece-wise constant reference signals," *IEEE Trans. Autom. Control*, vol. 63, no. 11, pp. 3735–3750, Nov. 2018.
[205] A. Domahidi, A. U. Zgraggen, M. N. Zeilinger, M. Morari, and C. N. Jones, "Efficient interior point methods for multistage problems arising in receding horizon control," in *Proc. IEEE Conf. Decis. Control*, Maui, HI, USA, Dec. 2012, pp. 668–674.

[206] J. Kalmari, J. Backman, and A. Visala, "A toolkit for nonlinear model predictive control using gradient projection and code generation," *Control Eng. Pract.*, vol. 39, pp. 56–66, 2015.
[207] F. Grimm, Z. Zhang, F. Wang, and R. Kennel, "Multistep predictive control of 3L-NPC power converters: Nonlinear branch-and-bound solution," in *Proc. Chin. Autom. Congr.*, Jinan, China, Oct. 2017, pp. 4678–4683.
[208] T. Geyer and N. Oikonomou, "Model predictive pulse pattern control with very fast transient responses," in *Proc. IEEE Energy Convers. Congr. Expo.*, Pittsburgh, PA, USA, Sep. 2014, pp. 5518–5524.
[209] T. Geyer, V. Spudic, W. van der Merwe, and E. Guidi, "Model predictive pulse pattern control of medium-voltage neutral-point-clamped inverter drives," in *Proc. IEEE Energy Convers. Congr. Expo.*, Portland, OR, USA, Sep. 2018, pp. 5047–5054.

Petros Karamanakos (S'10–M'14–SM'19) received the Diploma and the Ph.D. degrees in electrical and computer engineering from the National Technical University of Athens (NTUA), Athens, Greece, in 2007, and 2013, respectively.

From 2010 to 2011 he was with the ABB Corporate Research Center, Baden-Dättwil, Switzerland, where he worked on model predictive control strategies for medium-voltage drives. From 2013 to 2016 he was a PostDoc Research Associate in the Chair of Electrical Drive Systems and Power Electronics, Technische Universität München, Munich, Germany. Since September 2016, he has been an Assistant Professor in the Faculty of Information Technology and Communication Sciences, Tampere University, Tampere, Finland. His main research interests lie at the intersection of optimal control, mathematical programming and power electronics, including model predictive control for power electronic converters and ac drives.

Dr. Karamanakos received the 2014 Third Best Paper Award of the IEEE Transactions on Industry Applications and two Prize Paper Awards at conferences. He serves as an Associate Editor of the IEEE Transactions on Industry Applications and of the IEEE Open Journal of Industry Applications.

Eyke Liegmann (S'16) received the B.Sc. and M.Sc. degrees in electrical power engineering from RWTH Aachen University, Aachen, Germany, in 2013 and 2016, respectively. Currently he is pursuing the Dr.-Ing. degree at the Technical University of Munich, Munich, Germany.

In 2014, he worked as intern at ABB Corporate Research, Västeras, Sweden. From 2015 to 2016, he was with the Institute for Automation of Complex Power Systems-E.ON Energy Research Center-RWTH Aachen University. In 2018, he was visiting Ph.D. student at the Stellenbosch University, Stellenbosch, South Africa. In 2019, he visited Tampere University, Tampere, Finland. His interests are embedded control systems and model predictive control of electrical drive systems.

Mr. Liegmann received the Best Exhibition Award at the 2016 Power and Energy Student Summit and the 2019 Best Student Paper Award at the 2019 IEEE International Symposium on Predictive Control of Electrical Drives and Power Electronics.

Tobias Geyer (M'08–SM'10) received the Dipl.-Ing. and Ph.D. degrees in electrical engineering from ETH Zurich, Zurich, Switzerland, in 2000 and 2005, respectively, and the Habilitation degree in power electronics from ETH Zurich, Zurich, Switzerland, in 2017.

After his Ph.D., he spent three years at GE Global Research, Munich, Germany, three years at the University of Auckland, Auckland, New Zealand, and eight years at ABB's Corporate Research Centre, Baden-Dättwil, Switzerland. There, in 2016, he became a Senior Principal Scientist for power conversion control. He was appointed as an extraordinary Professor at Stellenbosch University, Stellenbosch, South Africa, from 2017 to 2020. In 2020, he joined ABB's medium-voltage drives business as R&D platform manager of the ACS6000/6080.

He is the author of 35 patent families and the book "Model predictive control of high power converters and industrial drives" (Wiley, 2016). He teaches a regular course on model predictive control at ETH Zurich. His research interests include medium-voltage and low-voltage drives, utility-scale power converters, optimized pulse patterns and model predictive control.

Dr. Geyer is the recipient of the 2017 First Place Prize Paper Award in the Transactions on Power Electronics, the 2014 Third Place Prize Paper Award in the Transactions on Industry Applications, and of two Prize Paper Awards at conferences. He is a former Associate Editor for the IEEE Transactions on Industry Applications (from 2011 until 2014) and the IEEE Transactions on Power Electronics (from 2013 until 2019). He was an international program committee vice chair of the IFAC conference on Nonlinear Model Predictive Control in Madison, WI, USA, in 2018. Dr. Geyer is a Distinguished Lecturer of the Power Electronics Society in the years 2020 and 2021.

Ralph Kennel (M'89–SM'96) received the Diploma and Dr.-Ing. (Ph.D.) degrees from the University of Kaiserslautern, Kaiserslautern, Germany, in 1979 and 1984, respectively.

From 1983 to 1999 he worked on several positions with Robert BOSCH GmbH, Germany. Until 1997, he was responsible for the development of servo drives. He was one of the main supporters of VECON and SERCOS interface, two multicompany development projects for a microcontroller and a digital interface especially dedicated to servo drives. Furthermore, he actively took part in the definition and release of new standards with respect to CE marking for servo drives. Between 1997 and 1999, he was responsible for "Advanced and Product Development of Fractional Horsepower Motors" in automotive applications. His main activity was preparing the introduction of brushless drive concepts to the automotive market. From 1994 to 1999, he was appointed Visiting Professor at the Newcastle University, Newcastle-upon-Tyne, U.K. From 1999 to 2008, he was Professor for Electrical Machines and Drives at the Wuppertal University, Wuppertal, Germany. Since 2008 he is Professor for Electrical Drive Systems and Power Electronics at Technische Universtät München, Munich, Germany. His main interests today are sensorless control of ac drives, predictive control of power electronics and hardware-in-the-loop systems.

Dr. Kennel is a Senior Member of IEEE, a Fellow of IET (former IEE) and a Chartered Engineer in the U.K. Within IEEE, he is Treasurer of the Germany Section as well as Distinguished Lecturer of the Power Electronics Society (IEEE-PELS). Dr. Kennel has received in 2013 the Harry Owen Distinguished Service Award from IEEE-PELS, the EPE Association Distinguished Service Award in 2015 as well as the 2019 EPE Outstanding Achievement Award. In 2018 Dr. Kennel received the Doctoral degree honoris causa from Universitatea Stefan cel Mare in Suceava (Romania). Dr. Kennel was appointed "Extraordinary Professor" by the University of Stellenbosch (South Africa) from 2016 to 2019 and as "Visiting Professor" at the Haixi Institute by the Chinese Academy of Sciences from 2016 to 2021.